Large eddy simulation and linear analysis of an airfoil in transitional flow: Insights on secondary tones and acoustic feedback







Tulio Ricciardi **William Wolf** **Kunihiko Taira**

University of Campinas

University of California Los Angeles

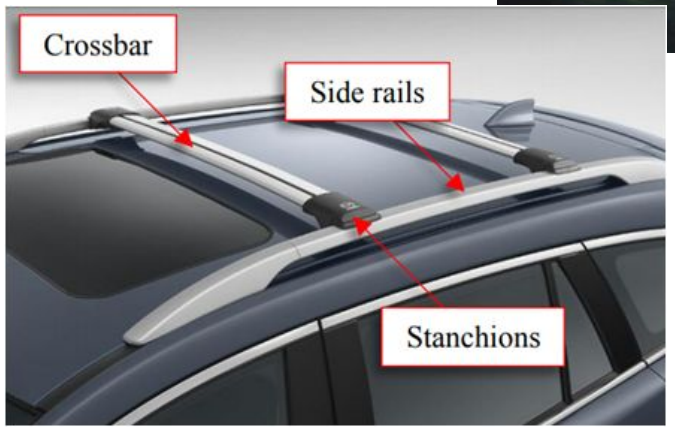
Advanced Modeling & Simulation (AMS) Seminar, June 10th, 2021

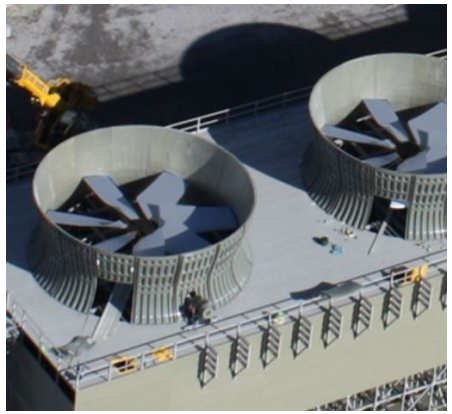
Airfoil noise







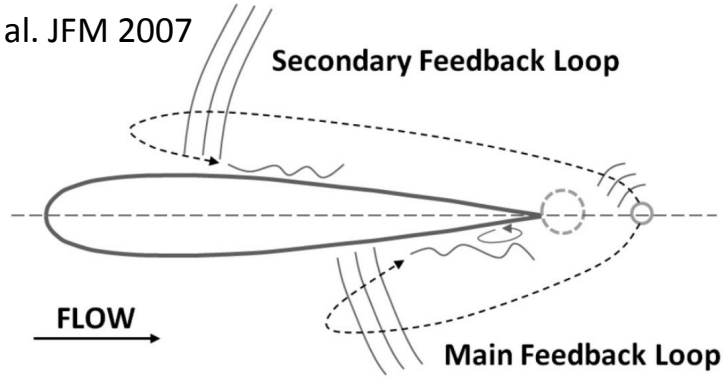


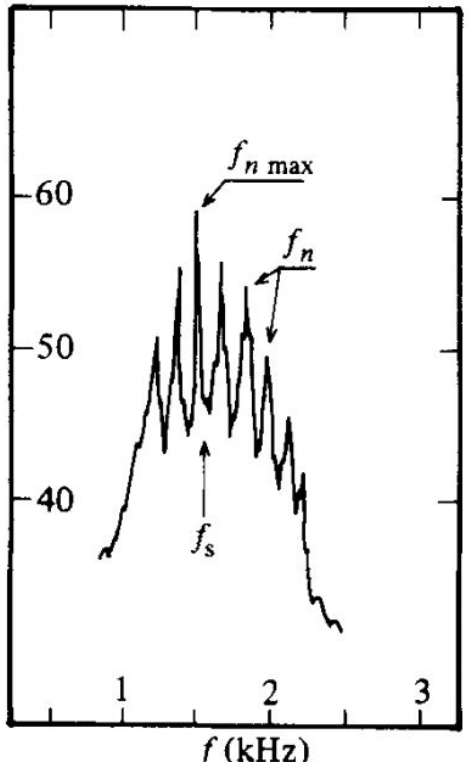


- Airfoil noise impacts the design of quieter transportation and energy devices
- Trailing-edge plays an important role
  - turbulent boundary layers: broadband spectrum
  - laminar boundary layers: narrowband spectrum (vortex shedding)
  - laminar-turbulent transition?
- Tonal noise generation studies at moderate Reynolds numbers: Paterson et al. 1973, Tam 1974, Fink 1975, Longhouse 1977, Arbey and Bataille 1983

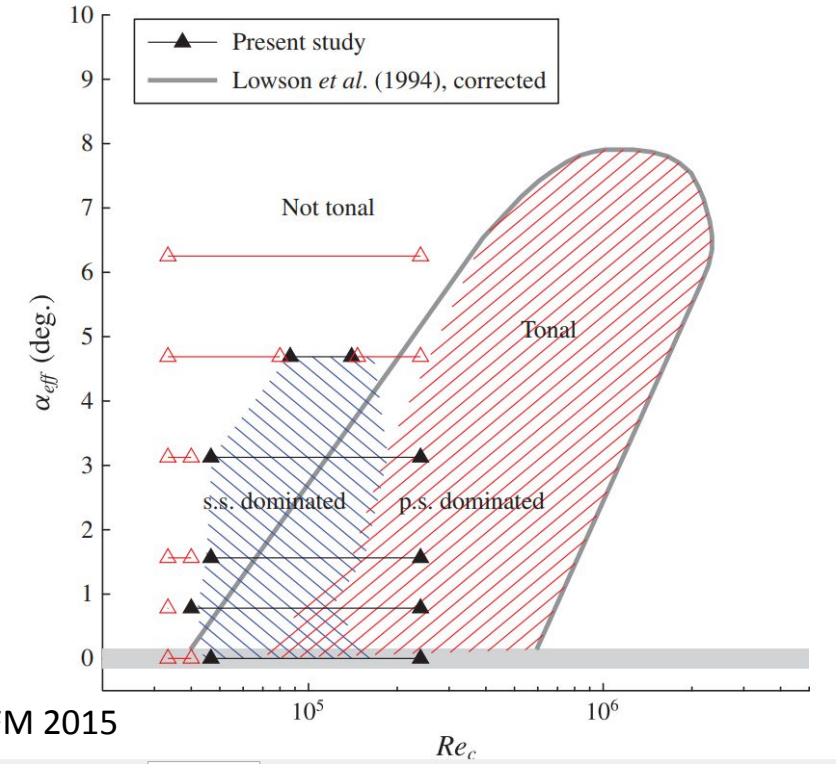
Airfoil noise

Desquesnes et al. JFM 2007





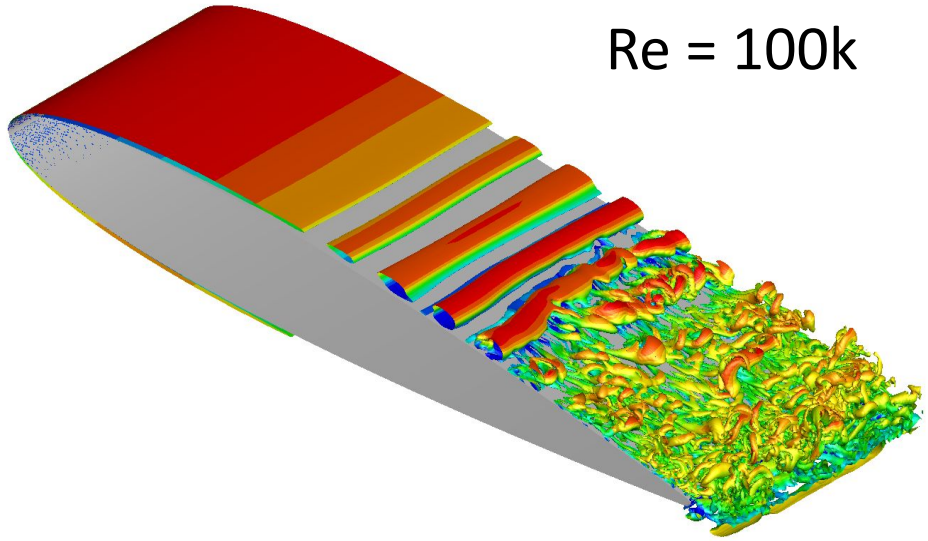
Arbey and Bataille JFM 1983

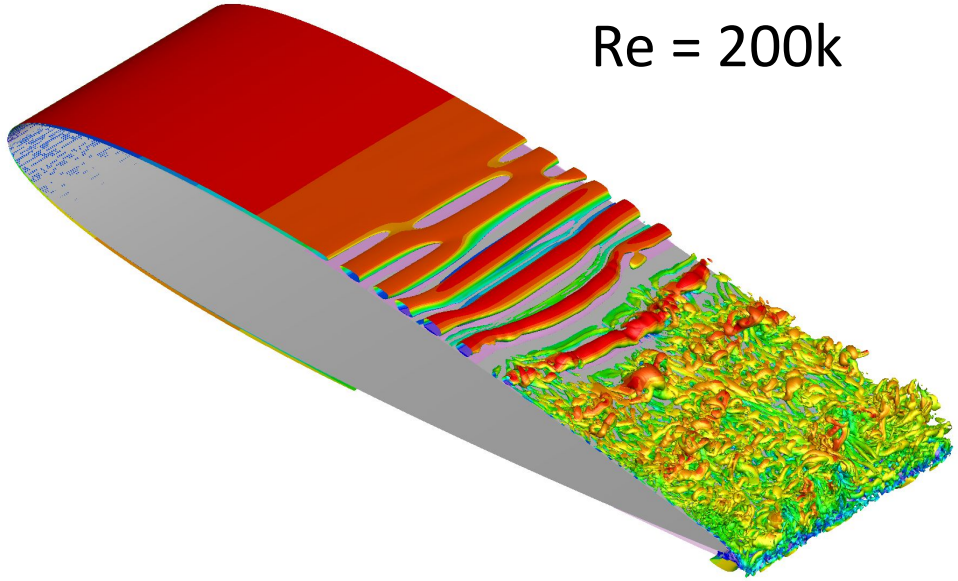


Probsting et al. JFM 2015

- Secondary tones related to scattering of TS-like waves (Arbey and Bataille 1983, Lowson 1994)
- Many authors discuss about an acoustic feedback loop mechanism
- Higher Reynolds numbers dominated by pressure side; lower Reynolds numbers dominated by suction side (Pröbsting et al. 2015)
- Separation bubbles appear either on pressure or suction sides
- Several open questions about both secondary tones and feedback

Airfoil noise

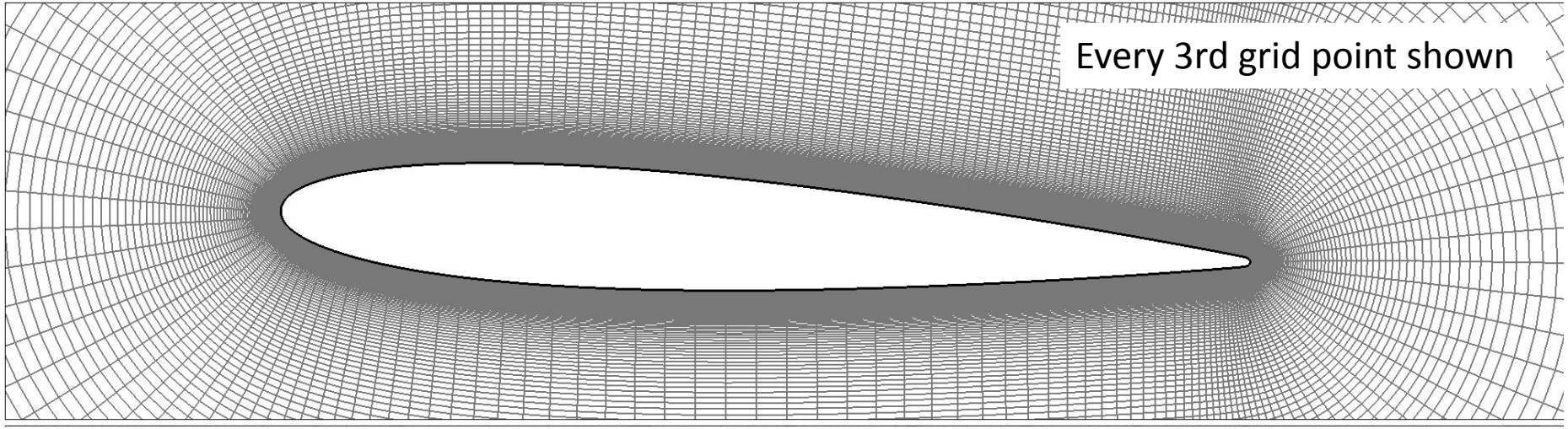




- Experiments show that pressure fluctuations are spanwise coherent
- Most numerical models are 2D (Desquesnes et al. 2007; Jones et al. 2008; Fosas de Pando et al. 2014 & 2017, Ricciardi et al. 2020)
- 2D models capture secondary tones but vortex dynamics is different
- Main objective of the present study:
  - investigate 3D effects on secondary tones and acoustic feedback loop
  - use linear analysis to gain insights on evolution of flow disturbances

Large eddy simulation (Re = 50,000; Ma = 0.3; AoA = 3 deg.)

- Compressible Navier Stokes equations solved in curvilinear coordinates [1]
- Spatial discretization: 6th-order compact finite difference + 6th-order compact interpolation on staggered grid [2]
- No explicit SGS model: 6-th order compact filter [3]
- Hybrid time marching: RK3 + Beam & Warming
- Airfoil: no-slip adiabatic b.c.
- Far-field: non-reflexive + sponge b.c.
- Span: periodical b.c. (z = 0.4c)
- (Nx, Ny, Nz) = (660, 600, 192) 76M points



[1] Nagarajan et al, JFM 2007

[2] Nagarajan et al, JCP 2003

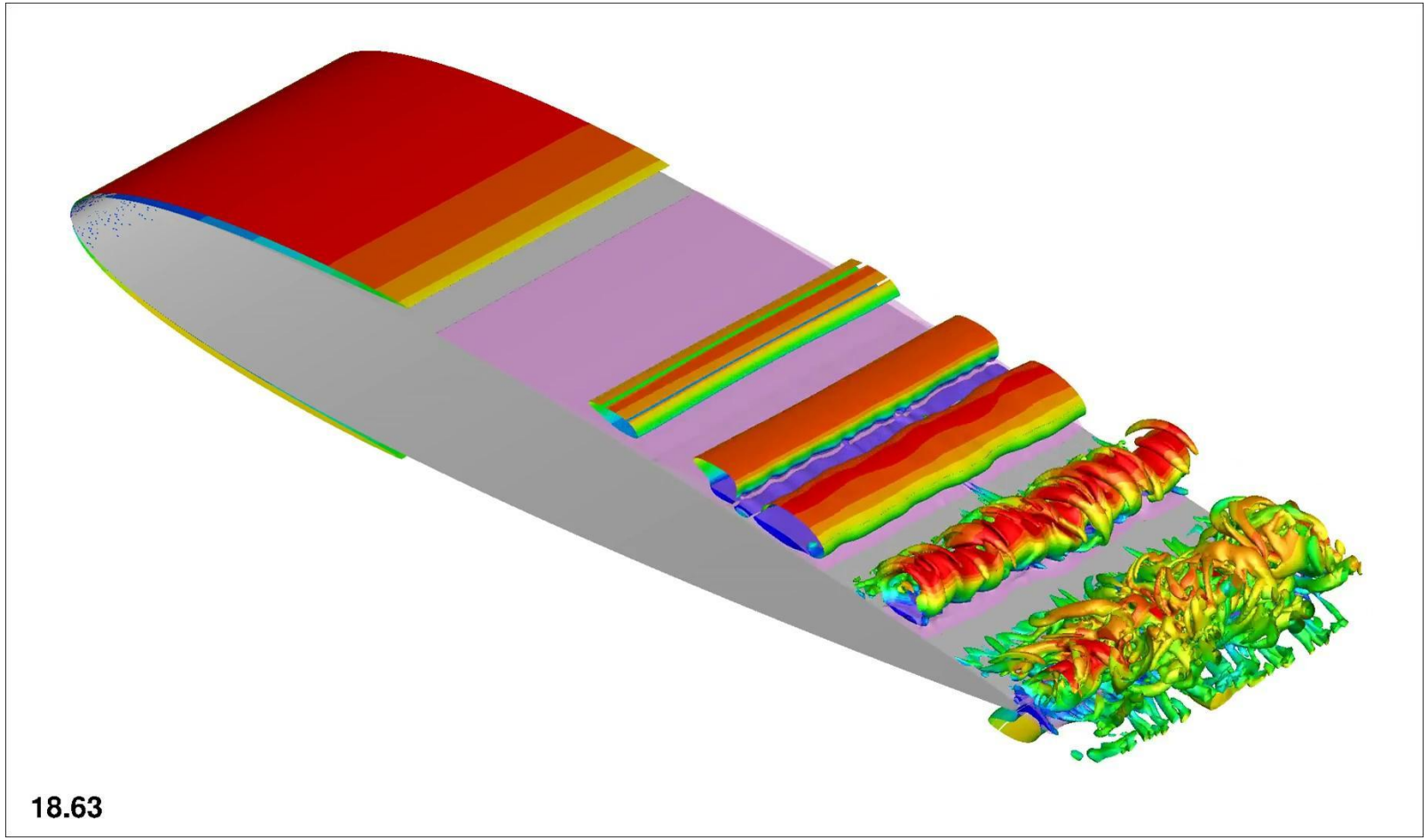
[3] Lele, JCP 1992

Flow characteristics

Iso-surfaces of q-criterion colored by u-velocity

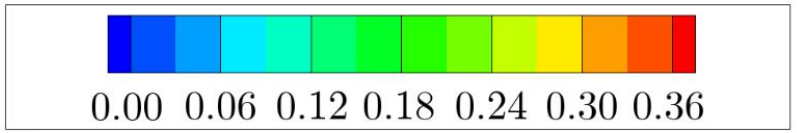
Surface in magenta color represents region of flow reversal

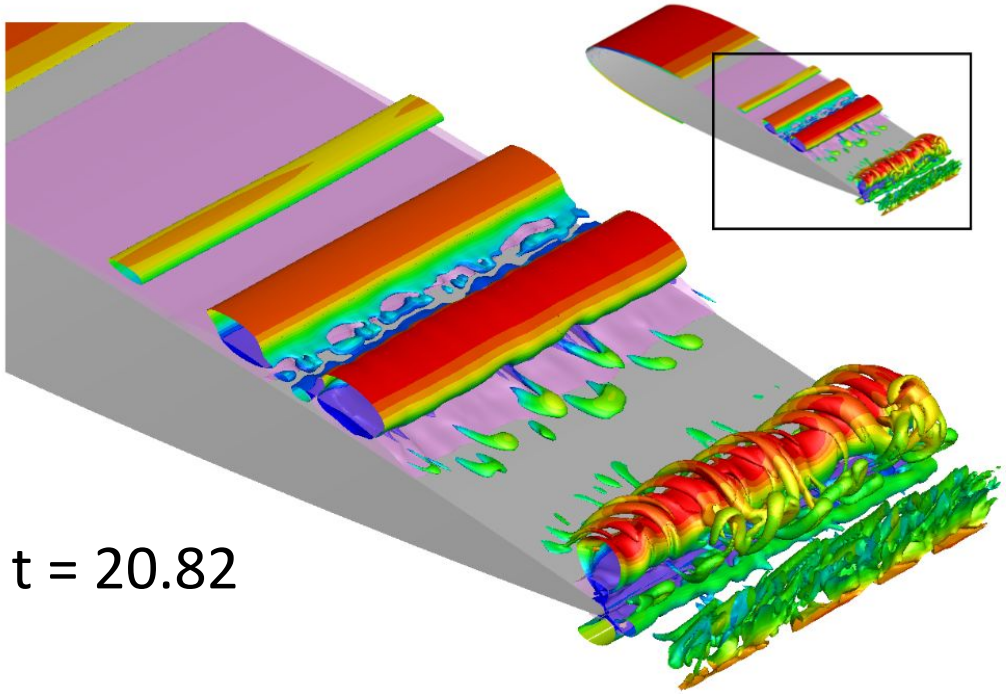
Notice unsteady separation

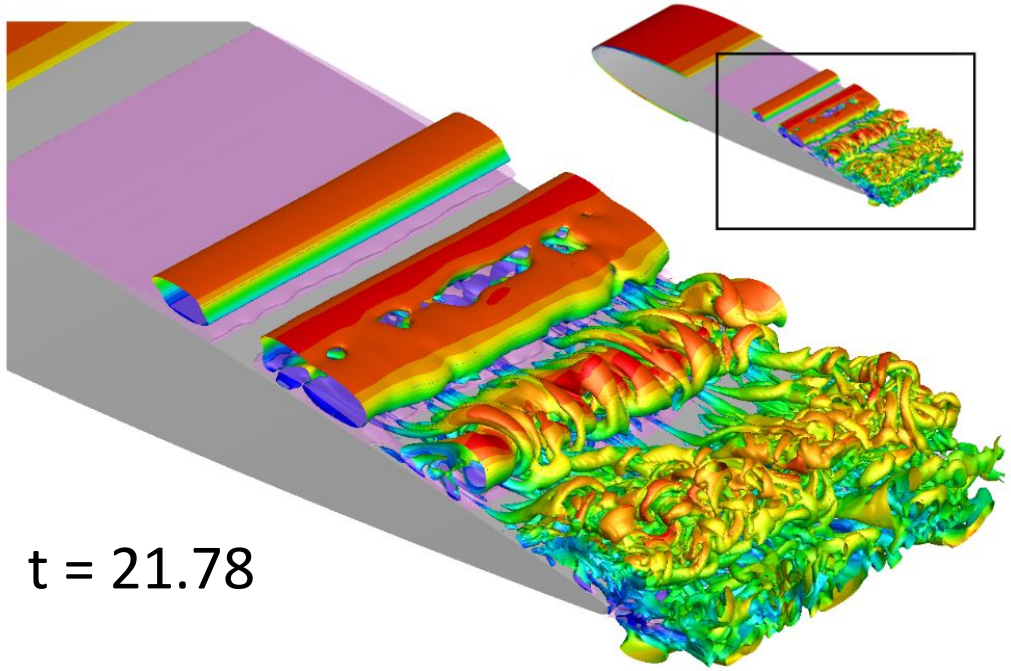


Flow characteristics

Iso-surfaces of q-criterion colored by u-velocity





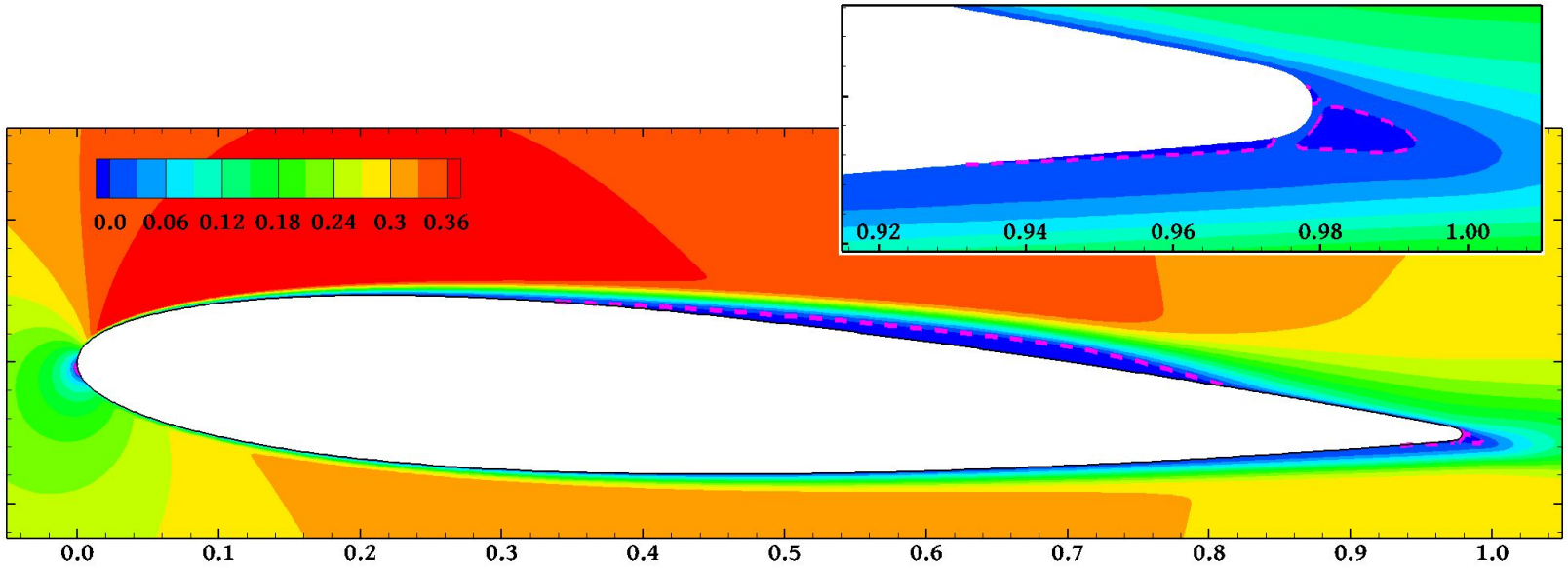


High spanwise coherence at the trailing edge

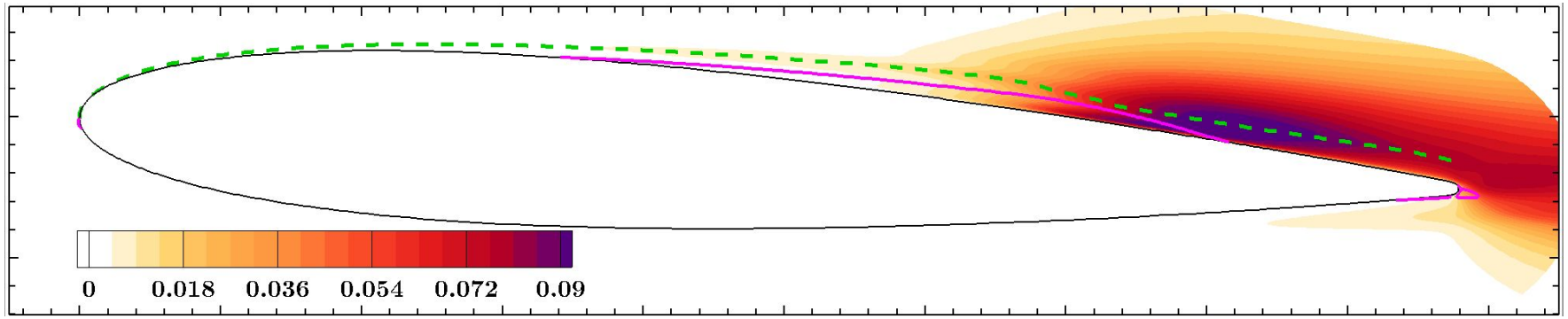
Low spanwise coherence at the trailing edge

Mean flow features

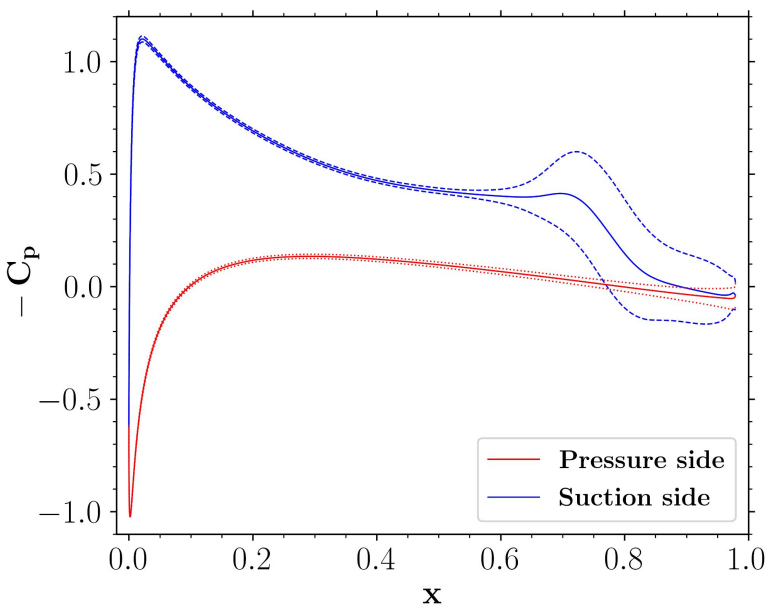
Mean u-velocity contours (magenta dashed line depicts reversed flow)



RMS values of kinetic energy (green dashed line shows location of maximum fluctuations)

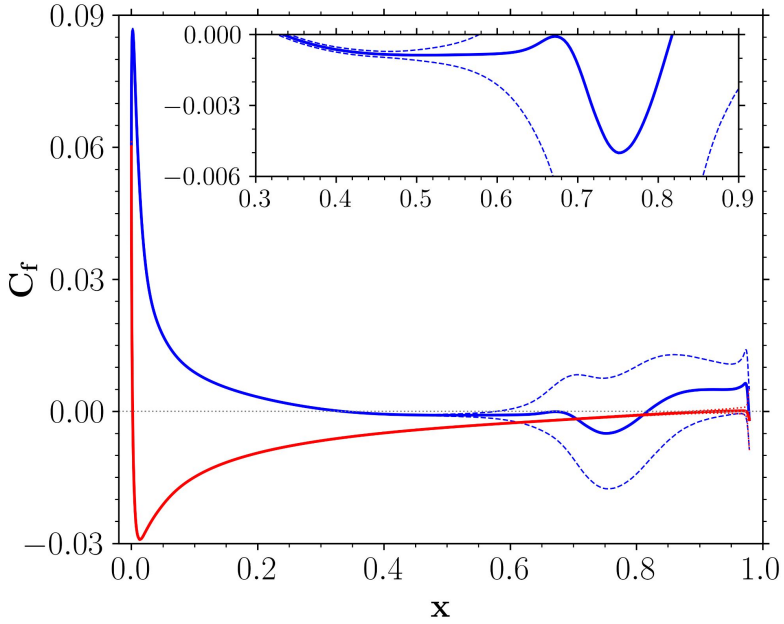


Mean flow features



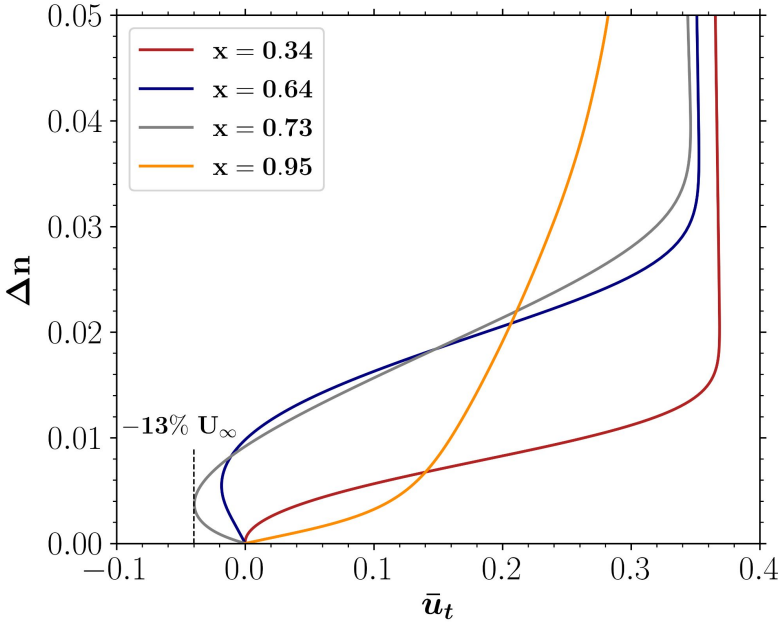
Cp = solid lines

Cp_{RMS} = dashed lines



Cf = solid lines

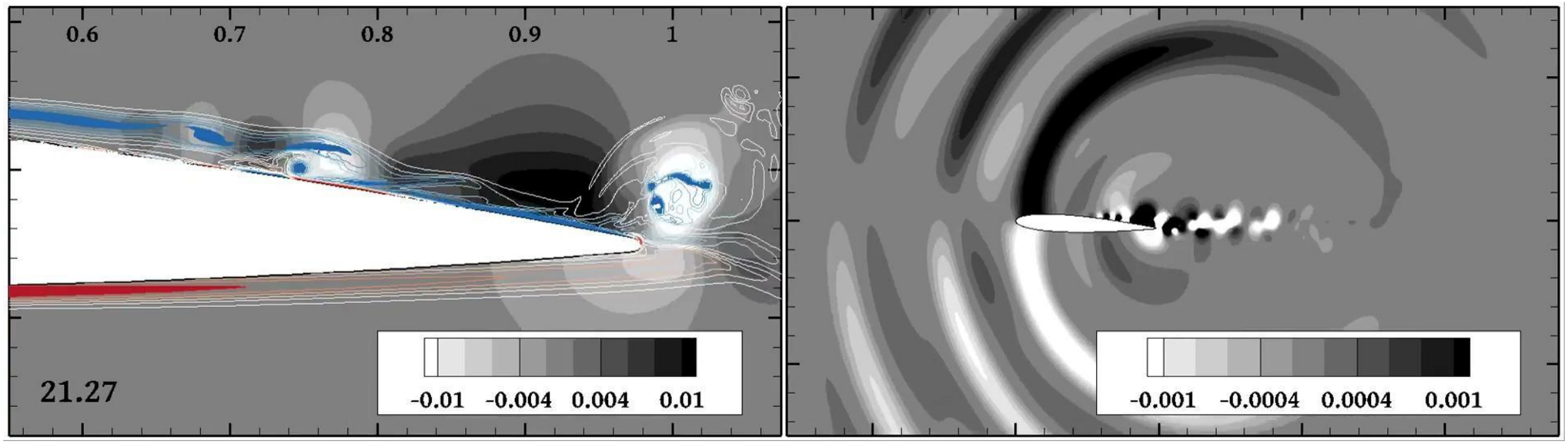
Cf_{RMS} = dashed lines



Mean tangential velocity profiles

Noise generation

Noise emission from trailing edge due acoustic scattering of boundary layer flow structures



Vorticity contours (color)

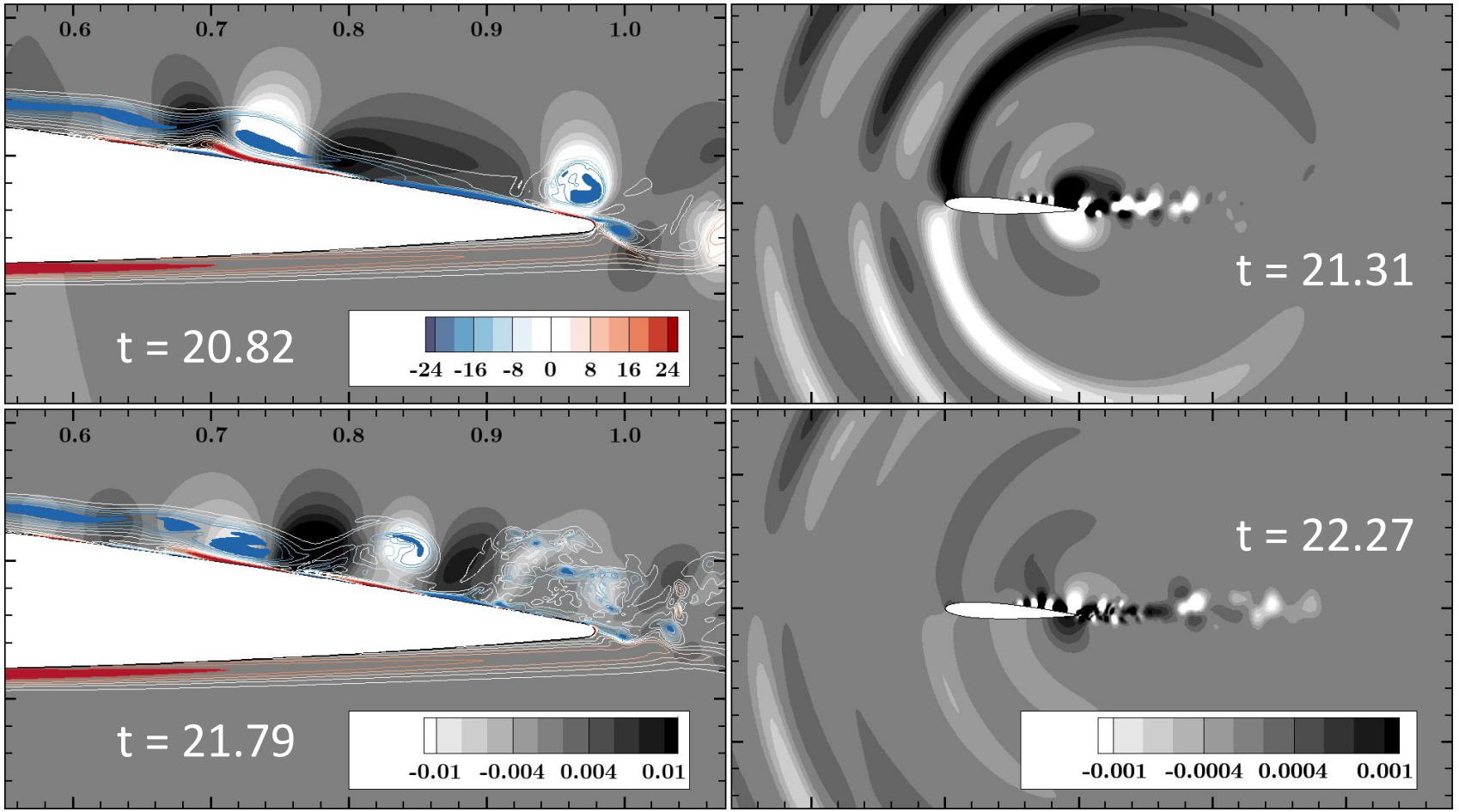
Hydrodynamic pressure fluctuations (gray scale)

Acoustic pressure fluctuations (gray scale)

Noise generation

Coherent structure near the trailing edge

Uncorrelated turbulence near the trailing edge

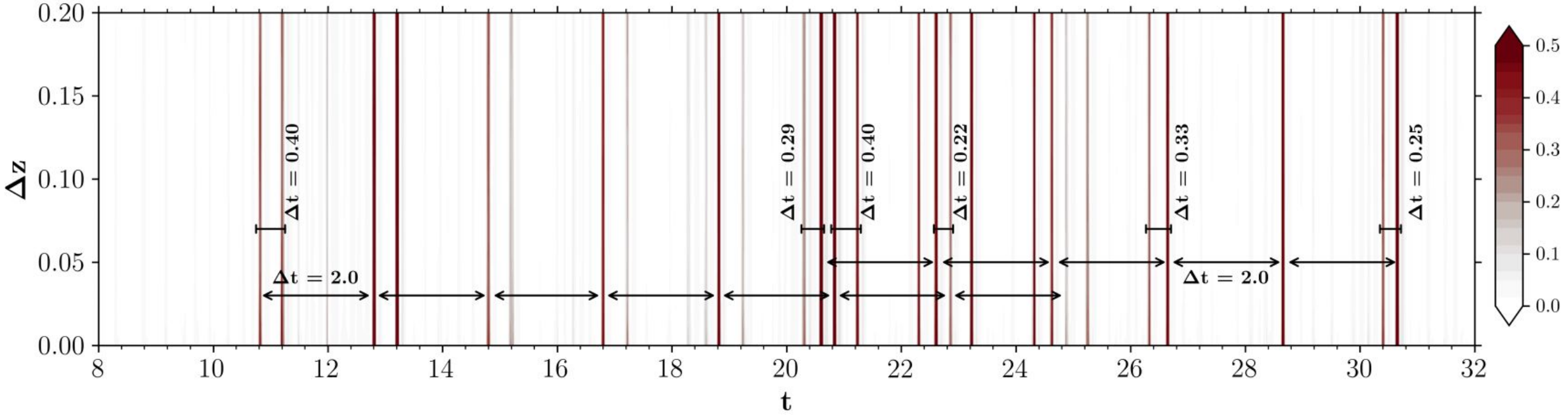


Near field: vorticity (color) and pressure fluctuations (gray)

Acoustic field: pressure fluctuations (gray)

Pressure correlation at the trailing edge

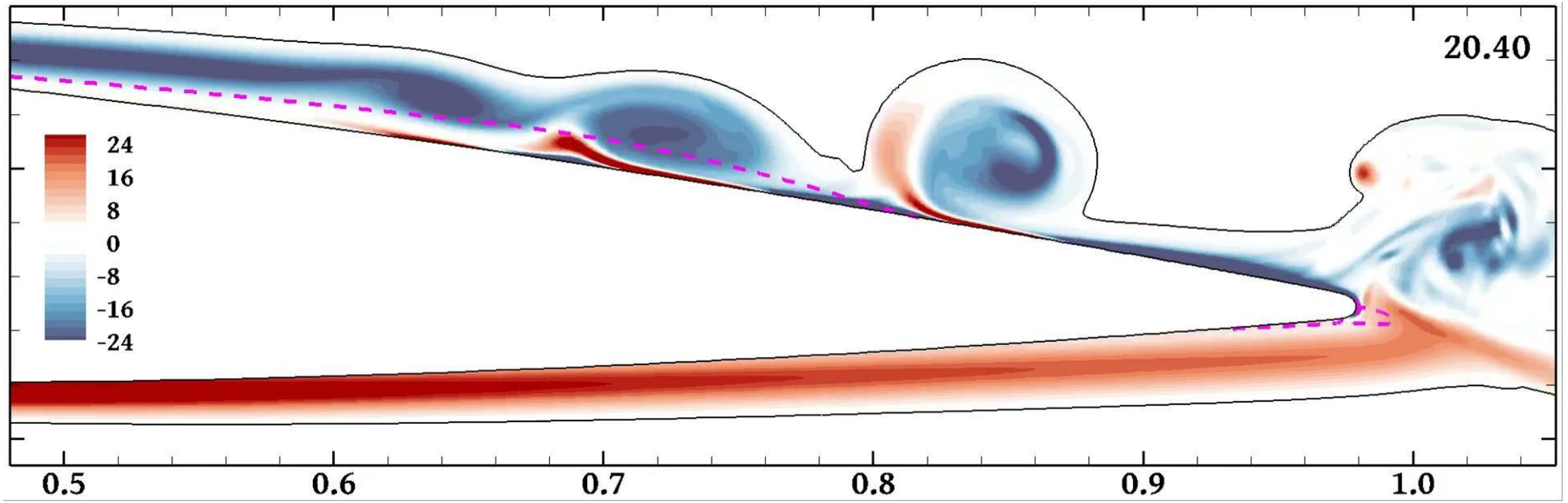
Two-point pressure correlation along airfoil span as function of time



- High correlation observed every 2 convective time units
- Intermittent events also observed at faster time scales

Vortex dynamics

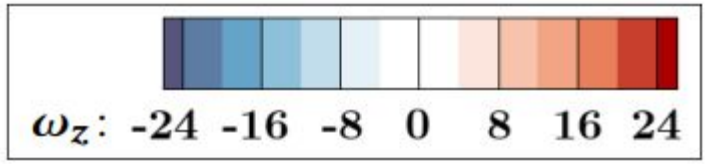
Spanwise averaged z-vorticity

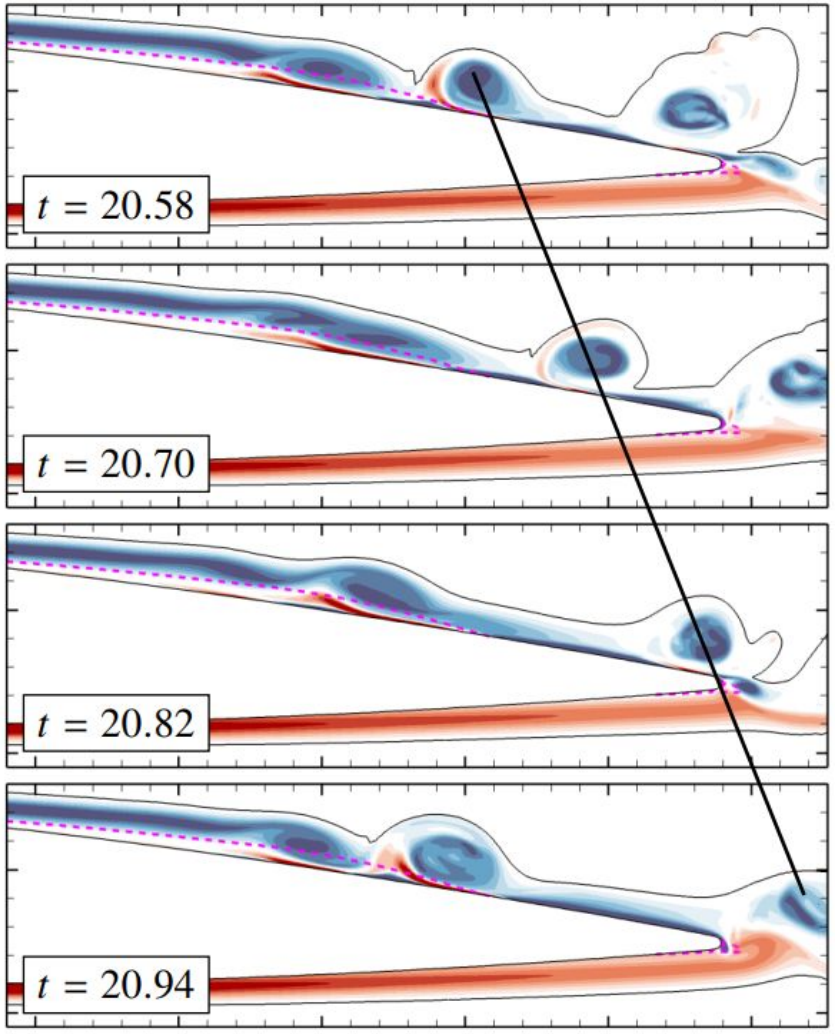


Thin black line represents an entropy measure (limit between rotational and irrotational flow)

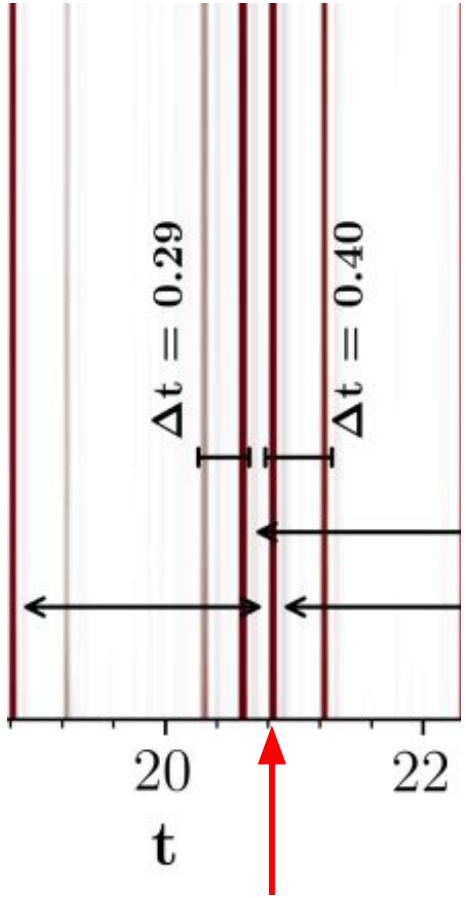
Vortex dynamics

Spanwise averaged z-vorticity





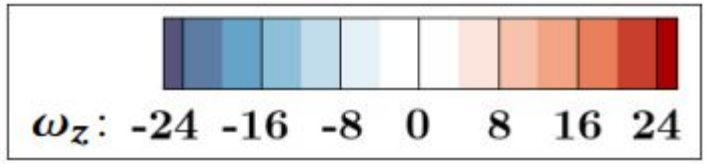
Case 1: Solitary vortex keeps high coherence

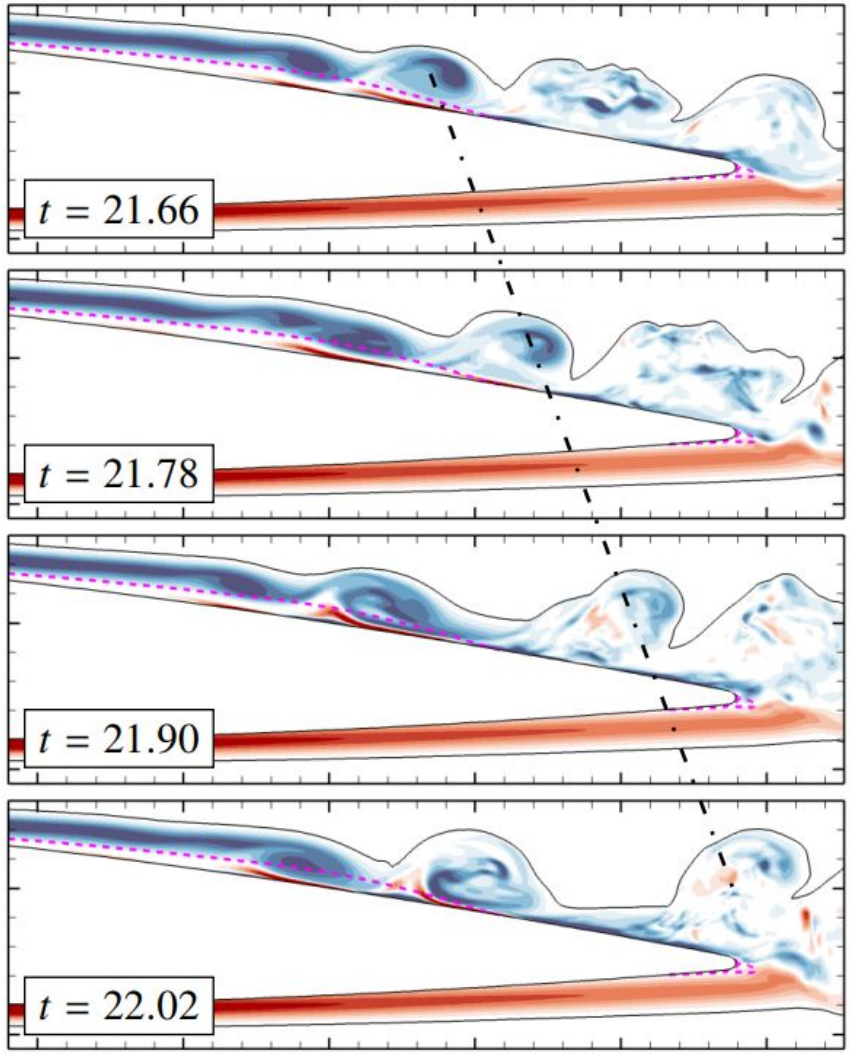


Two-point pressure correlation (spanwise) at trailing edge

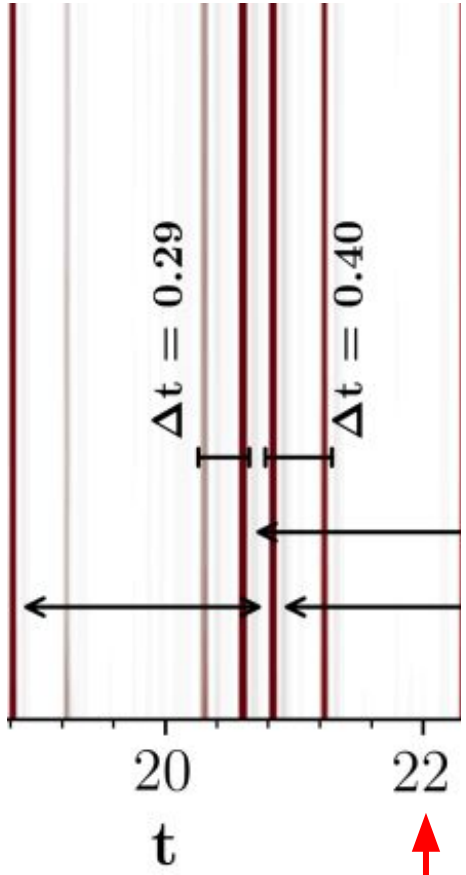
Vortex dynamics

Spanwise averaged z-vorticity





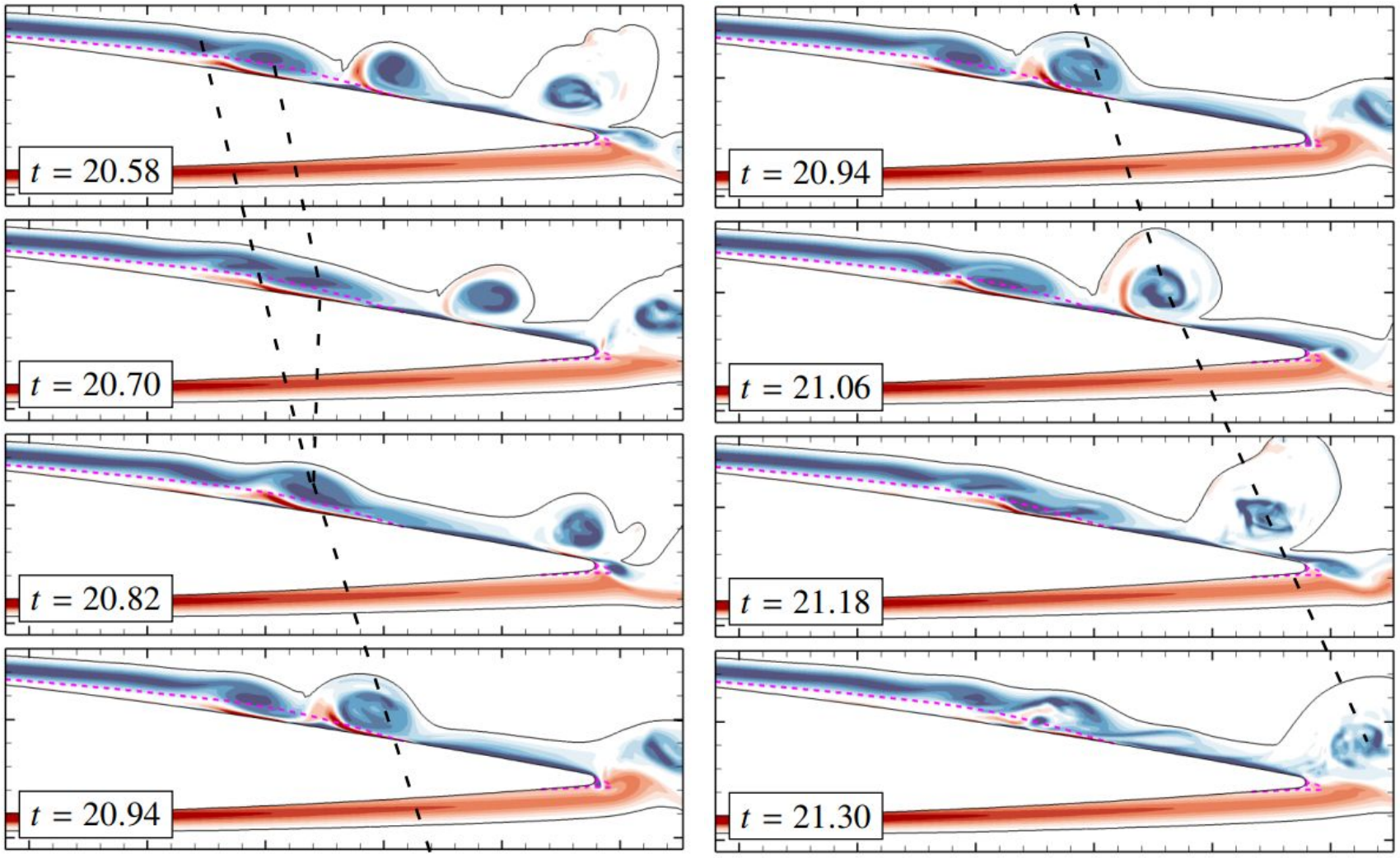
Case 2: Vortex bursting reduces coherence

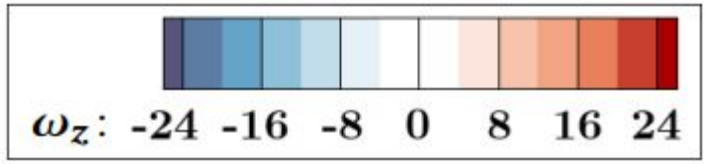


Two-point pressure correlation (spanwise) at trailing edge

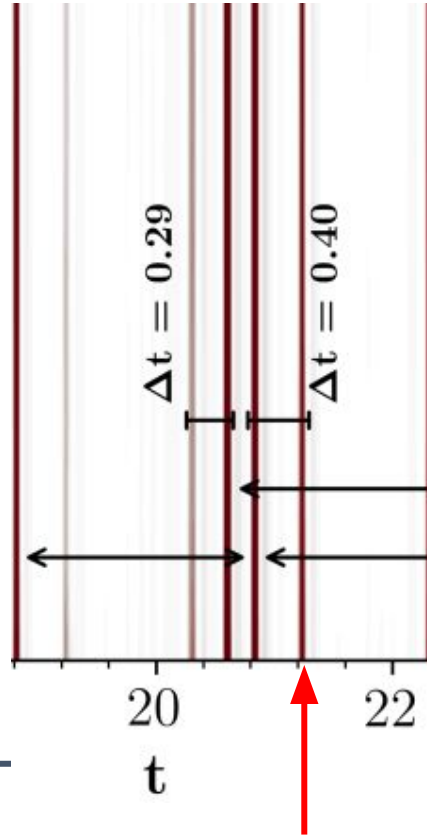
Vortex dynamics

Spanwise averaged z-vorticity

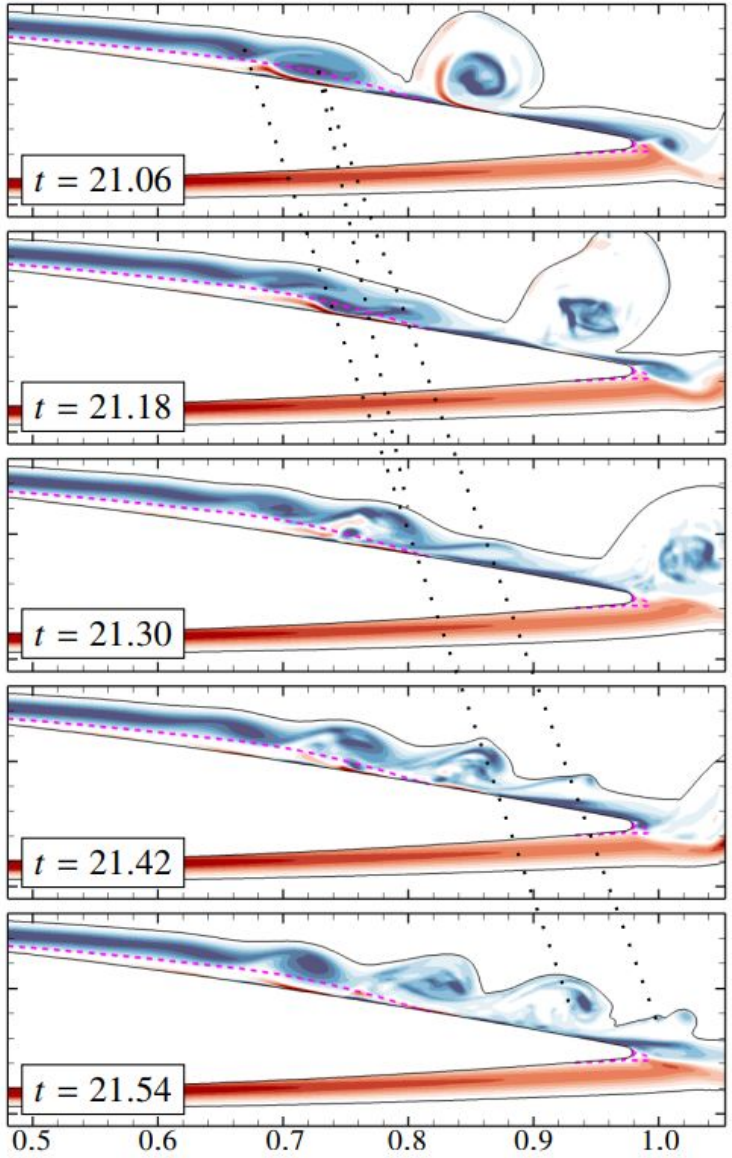




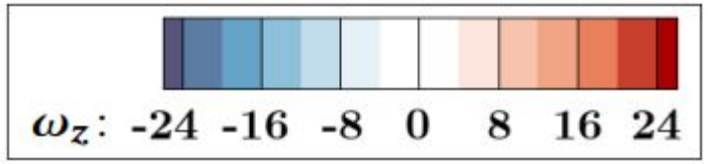
Case 3: Vortex merging keeps high coherence



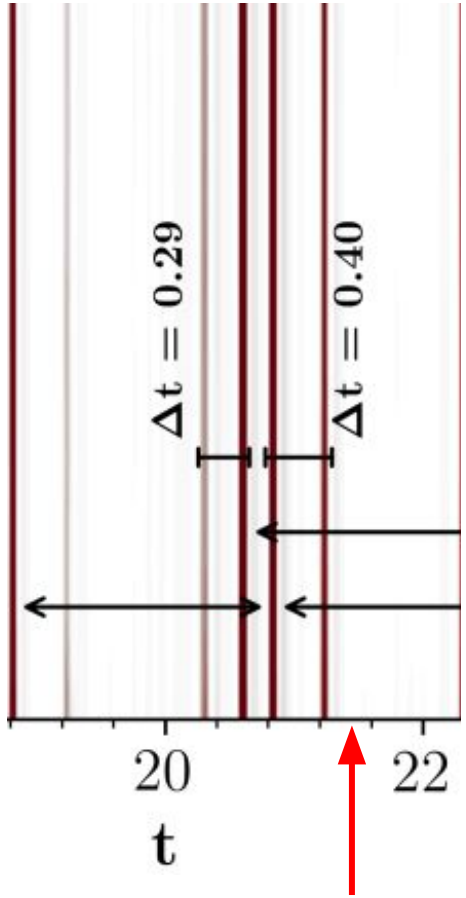
Vortex dynamics



Spanwise averaged z-vorticity

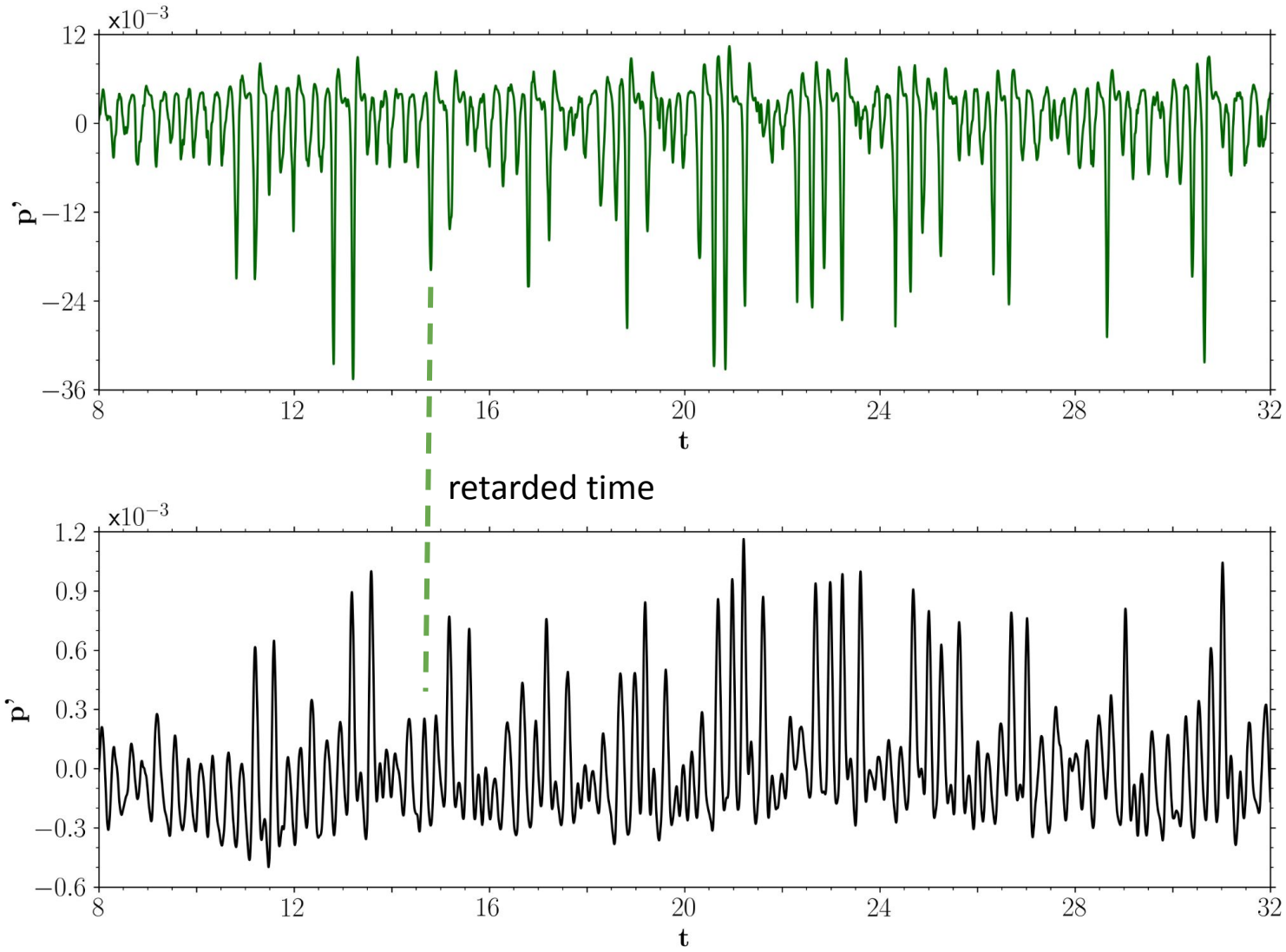


Case 4: Vortex merging is not successful and coherence is reduced



Two-point pressure correlation (spanwise) at trailing edge

Pressure fluctuation signals



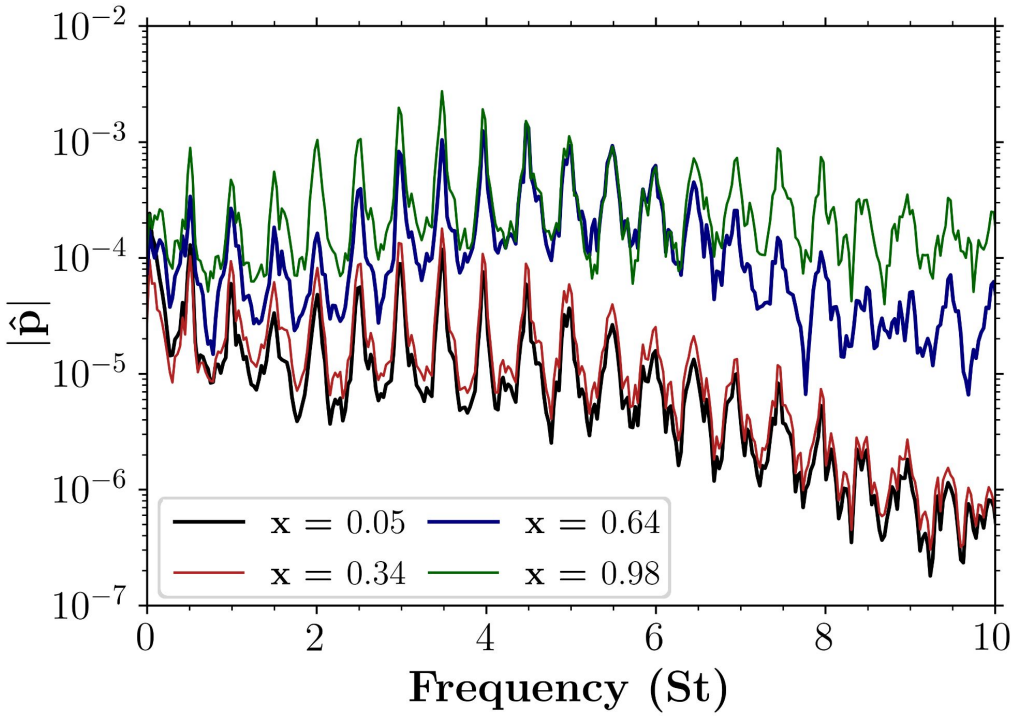
Airfoil surface at the trailing edge

Low pressure disturbances from coherent vortices

Acoustic near-field one chord above the trailing edge

Negative pulses at TE radiate positive acoustic waves

Spectral analysis



Pressure spectra at different chord positions

FFTs computed with 67% overlap; 4 bins; Hanning window; freq. resolution = 0.03

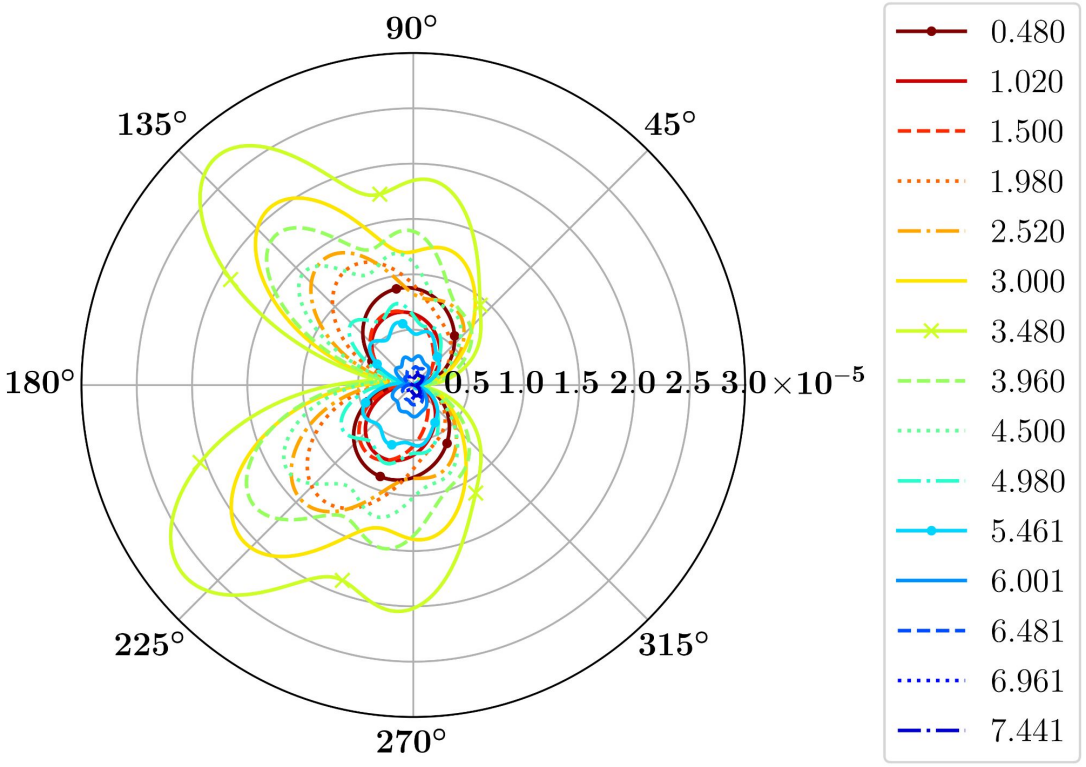
- ➔ x = 0.05 (leading edge): dominant tone at St ~ 3.5
- ➔ x = 0.34 (detachment point): dominant tone at St ~ 3.5
- ➔ x = 0.64 (shear layer roll-up region): dominant tone at St ~ 4.5
- ➔ x = 0.98 (trailing edge): dominant tone at St ~ 3.5

Upstream acoustic disturbances reach x = 0.05 and x = 0.34

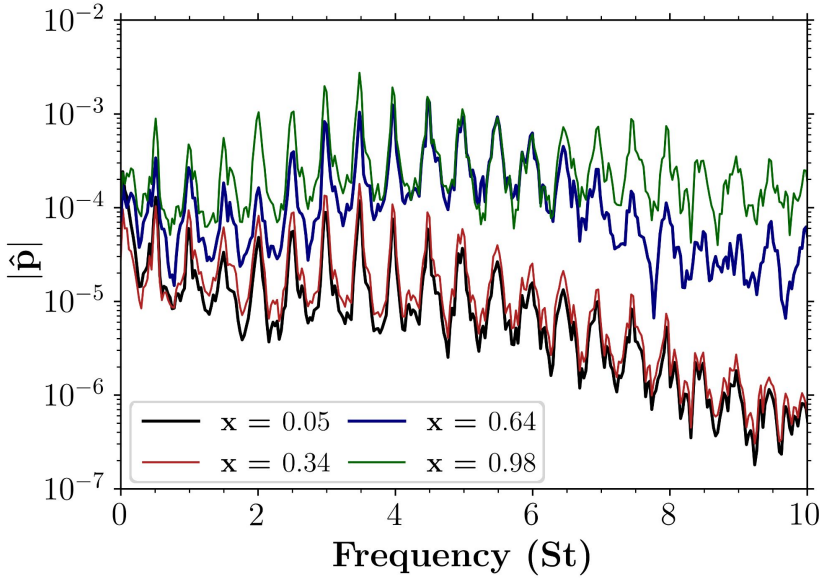
Primary flow structures (before merging) have higher frequencies at x = 0.64

After merging, St ~ 3.5 at the trailing edge

Spectral analysis

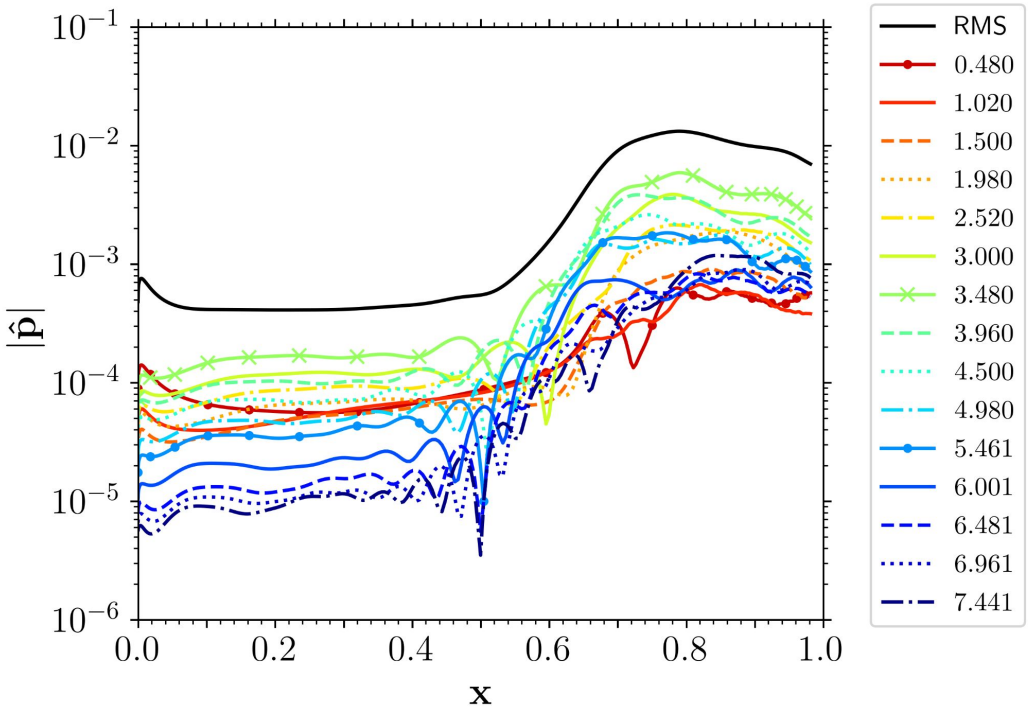


Sound directivities at 5 chords from TE
(different tonal frequencies in color)



Noise emission
dominated by St ~ 3.5
(main tone)

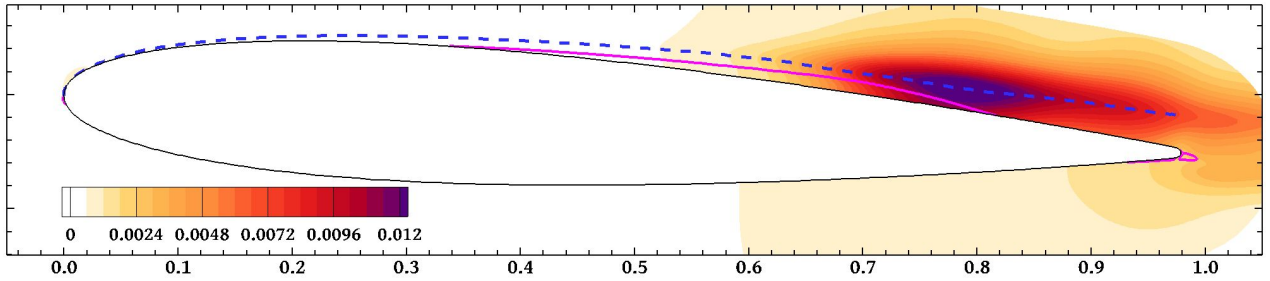
Spectral analysis

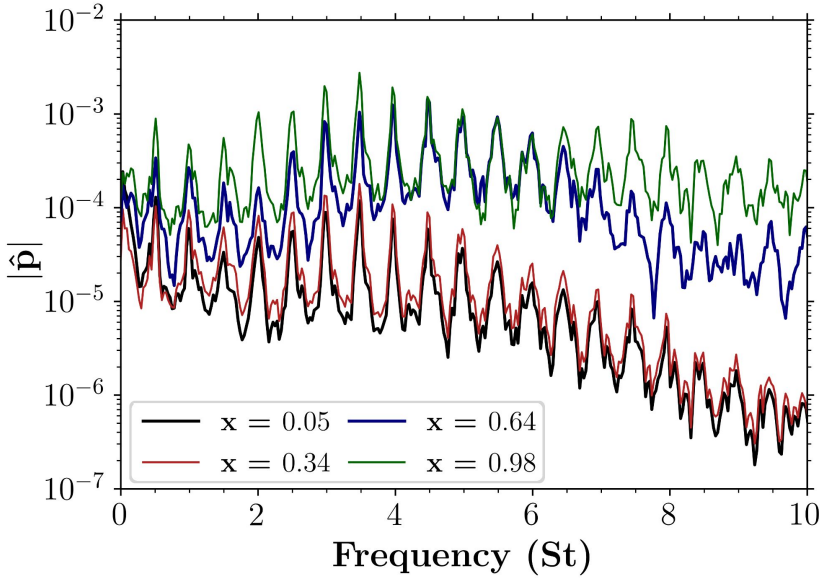


Magnitude of pressure Fourier coefficients (different tonal frequencies in color)

- Plateau upstream separation bubble
  - Exponential growth along bubble
- Saturation downstream reattachment

Probes located along dashed blue line



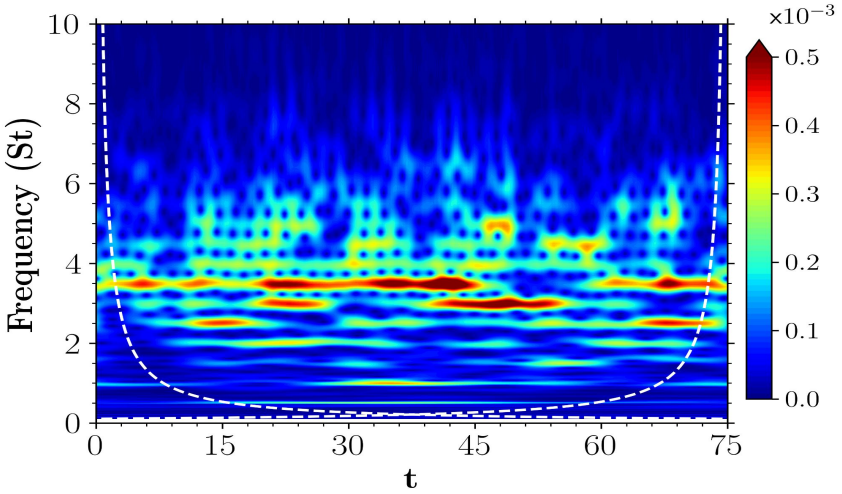


Time-frequency analysis (intermittency effects)

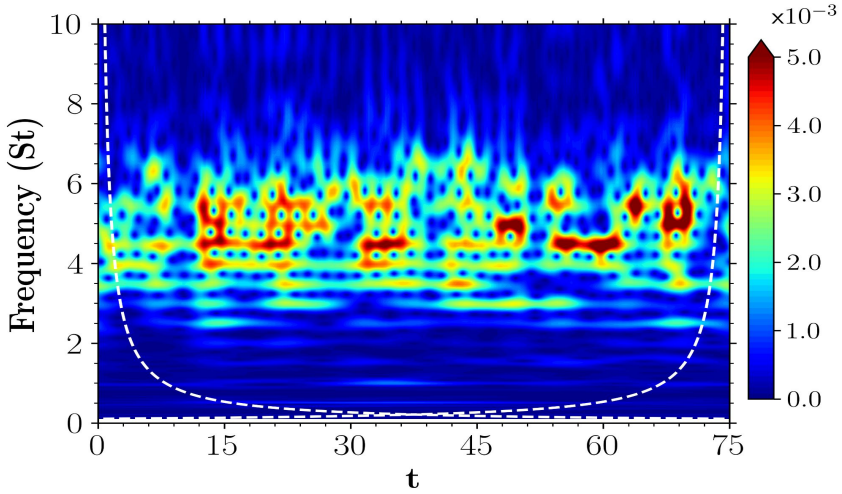
Continuous wavelet transform (Morlet wavelet)

Note the different levels!

Surface pressure fluctuations at x = 0.34 (detachment point)



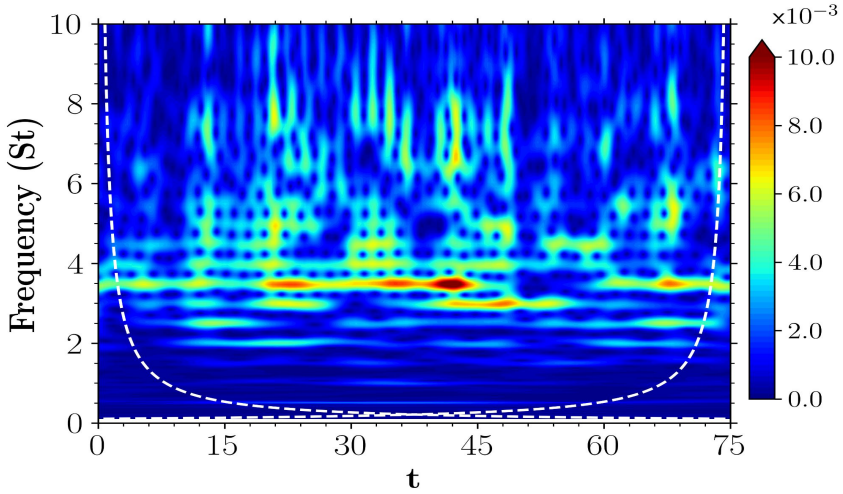
St ~ 3.5 dominates



Surface pressure fluctuations at x = 0.64 (shear layer roll-up)

St ~ 4.5 dominates

Surface pressure fluctuations at x = 0.98 (trailing edge)



St ~ 3.5 dominates

Linear stability analysis

- Linearized Navier Stokes equations

$$\frac{\partial \boldsymbol{q}'}{\partial t} = \boldsymbol{\mathcal{L}} \boldsymbol{q}'$$

- Fourier decomposition in span
- Laplace transform in time

$$\bullet'(x, y, z, t) = \int_{-\infty}^{\infty} \int_{-\infty}^{\infty} \hat{\bullet}(x, y, \beta, \omega) e^{\mathrm{i}(\beta z - \omega t)} \, d\beta \, d\omega$$

- Bi-global stability analysis

$$-\mathrm{i}\omega \hat{\boldsymbol{q}} = \boldsymbol{L} \hat{\boldsymbol{q}}$$

- Eigenvalue problem

$$\boldsymbol{Q\Lambda} = \boldsymbol{LQ}$$

Linear stability analysis

- Linearized Navier Stokes equations

$$\frac{\partial \boldsymbol{q}'}{\partial t} = \mathcal{L}\boldsymbol{q}'$$

- Fourier decomposition in span
- Laplace transform in time

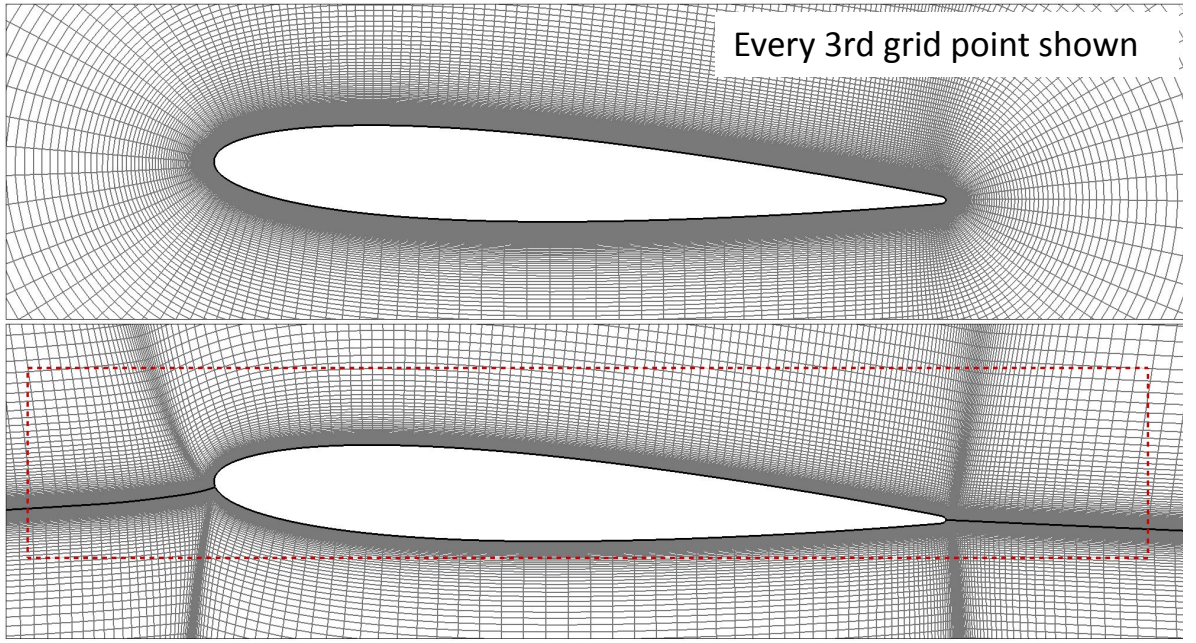
$$\bullet'(x, y, z, t) = \int_{-\infty}^{\infty}\int_{-\infty}^{\infty} \hat{\bullet}(x, y, \beta, \omega) e^{\mathrm{i}(\beta z - \omega t)}\, d\beta\, d\omega$$

- Bi-global stability analysis

$$-\mathrm{i}\omega\hat{\boldsymbol{q}} = \boldsymbol{L}\hat{\boldsymbol{q}}$$

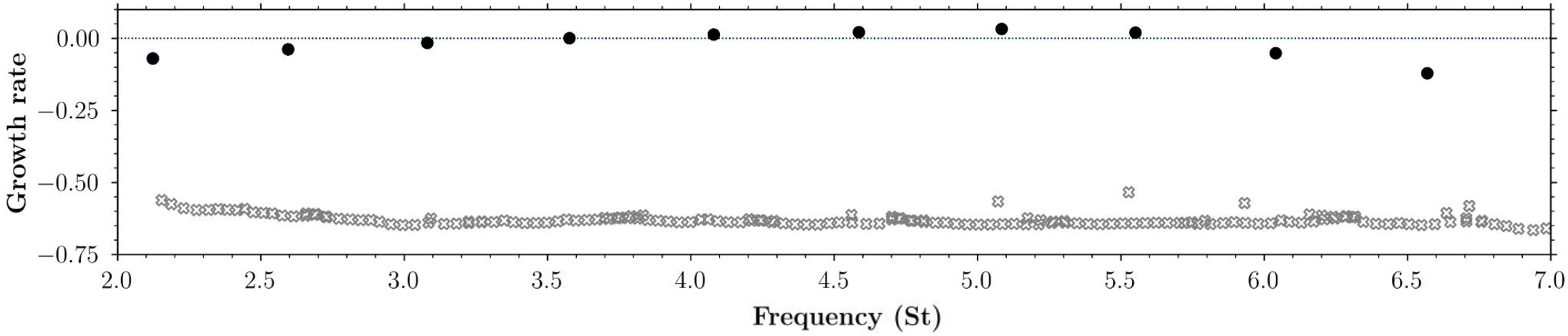
- Eigenvalue problem

$$\boldsymbol{Q}\boldsymbol{\Lambda} = \boldsymbol{L}\boldsymbol{Q}$$



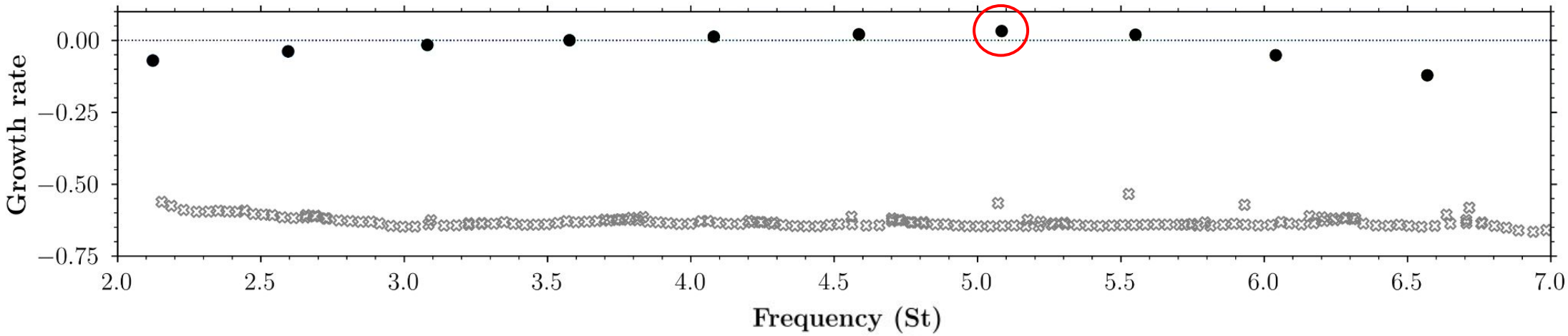
- Mean flow interpolated from structured O-grid to unstructured H-grid
- H-grid: 520k points
- Cut-off frequency: St = 8.0
- Circular sponge centered at mid-chord
- Sun et al. JFM 2017; Yeh and Taira JFM 2019

Linear stability analysis

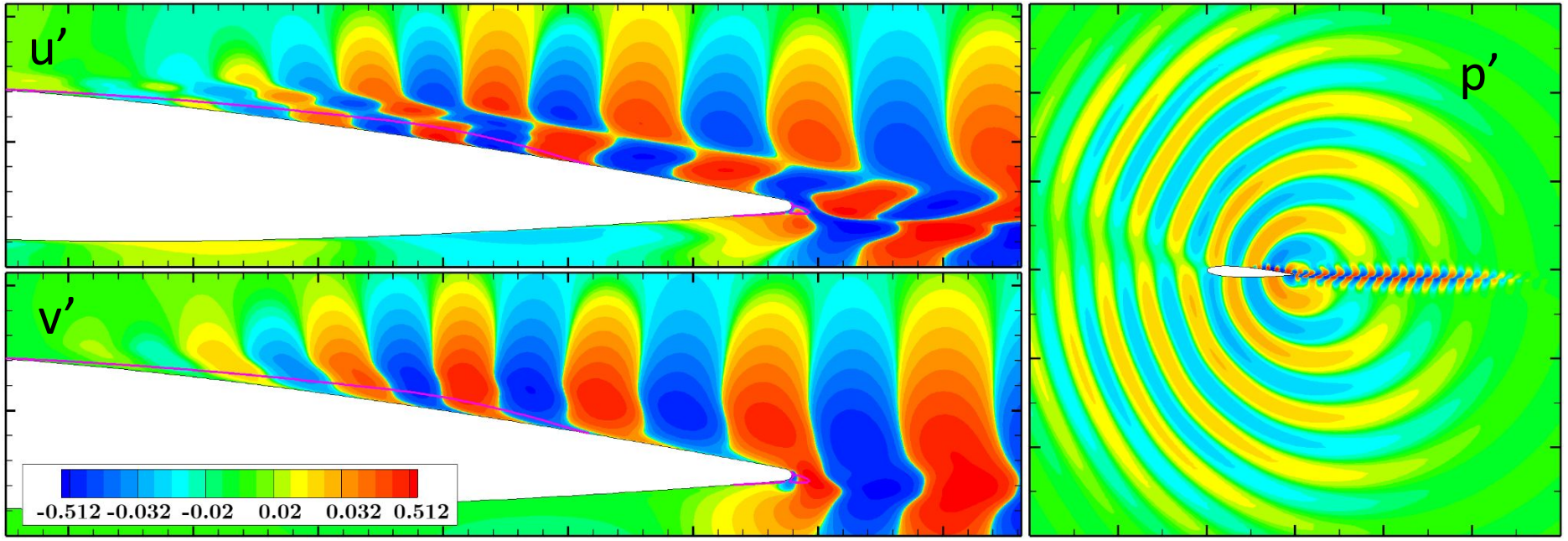


- Marginally stable and unstable modes

Linear stability analysis



- Marginally stable and unstable modes (β = 0)
- Most amplified global mode at St ~ 5.1



Resolvent analysis

- Linearized Navier Stokes equations w/ forcing

$$\frac{\partial \boldsymbol{q}'}{\partial t} = \mathcal{L}\boldsymbol{q}' + \mathcal{B}\boldsymbol{f}'$$

- State-space representation

$$-\mathrm{i}\omega\hat{\boldsymbol{q}} = \boldsymbol{L}\hat{\boldsymbol{q}} + \boldsymbol{B}\hat{\boldsymbol{f}} \qquad \hat{\boldsymbol{y}} = \boldsymbol{C}\hat{\boldsymbol{q}}$$

- Resolvent operator $\boldsymbol{H}(\bar{\boldsymbol{q}}, \beta, \tilde{\omega})$

$$\hat{\boldsymbol{q}} = (-\mathrm{i}\tilde{\omega}\boldsymbol{I} - \boldsymbol{L})^{-1}\boldsymbol{B}\hat{\boldsymbol{f}} = \boldsymbol{H}\,\boldsymbol{B}\hat{\boldsymbol{f}}$$

- Input-output analysis
- Modified resolvent operator (energy norm)

$$\boldsymbol{H}_w = \boldsymbol{W}\boldsymbol{C}(-\mathrm{i}\tilde{\omega}\boldsymbol{I} - \boldsymbol{L})^{-1}\boldsymbol{B}\boldsymbol{W}^{-1}$$

$$\boldsymbol{H}_w = \boldsymbol{U}\boldsymbol{\Sigma}\boldsymbol{V}^{*}$$ Max singular value

Resolvent analysis

- Linearized Navier Stokes equations w/ forcing

$$\frac{\partial q'}{\partial t} = \mathcal{L}q' + \mathcal{B}f'$$

- State-space representation

$$-\mathrm{i}\omega\hat{q} = \boldsymbol{L}\hat{q} + \boldsymbol{B}\hat{f} \qquad \hat{y} = \boldsymbol{C}\hat{q}$$

- Resolvent operator $\boldsymbol{H}(\bar{q}, \beta, \tilde{\omega})$

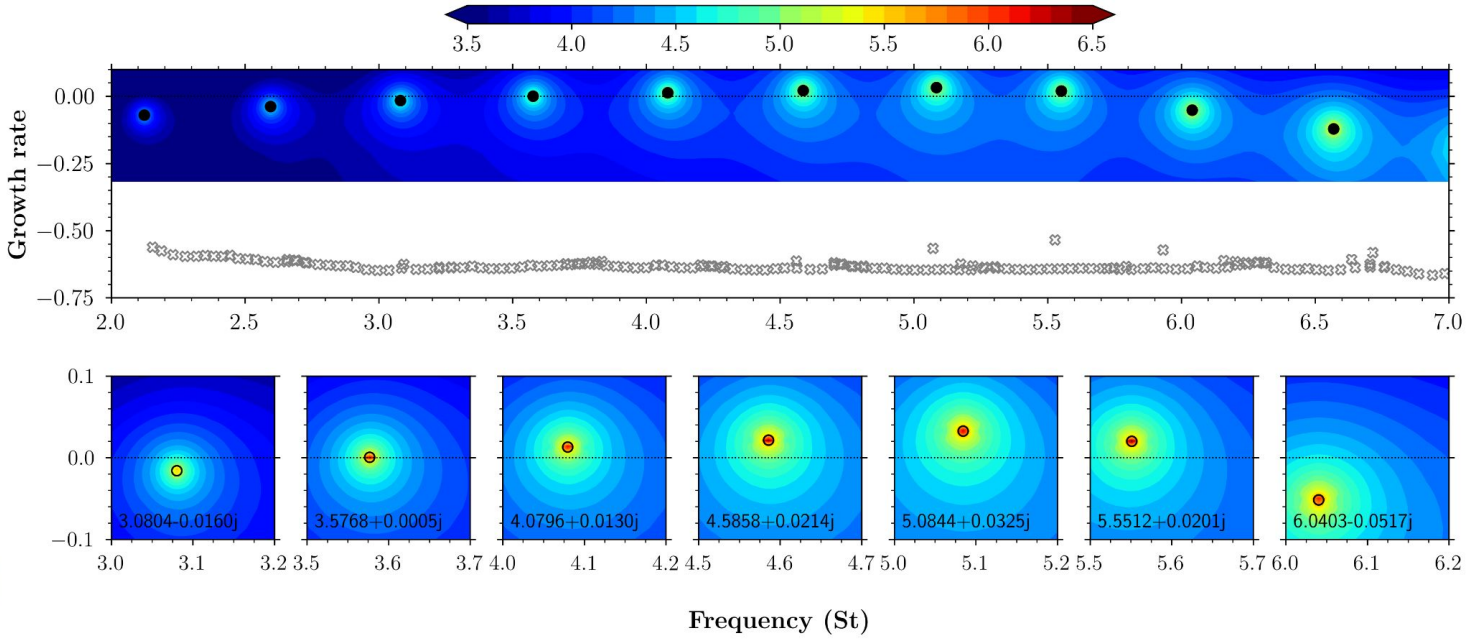
$$\hat{q} = (-\mathrm{i}\tilde{\omega}\boldsymbol{I} - \boldsymbol{L})^{-1}\boldsymbol{B}\hat{f} = \boldsymbol{H}\,\boldsymbol{B}\hat{f}$$

- Input-output analysis
- Modified resolvent operator (energy norm)

$$\boldsymbol{H}_w = \boldsymbol{W}\boldsymbol{C}(-\mathrm{i}\tilde{\omega}\boldsymbol{I} - \boldsymbol{L})^{-1}\boldsymbol{B}\boldsymbol{W}^{-1}$$

$$\boldsymbol{H}_w = \boldsymbol{U}\boldsymbol{\Sigma}\boldsymbol{V}^{*}$$ Max singular value

Pseudospectrum (log-scale)



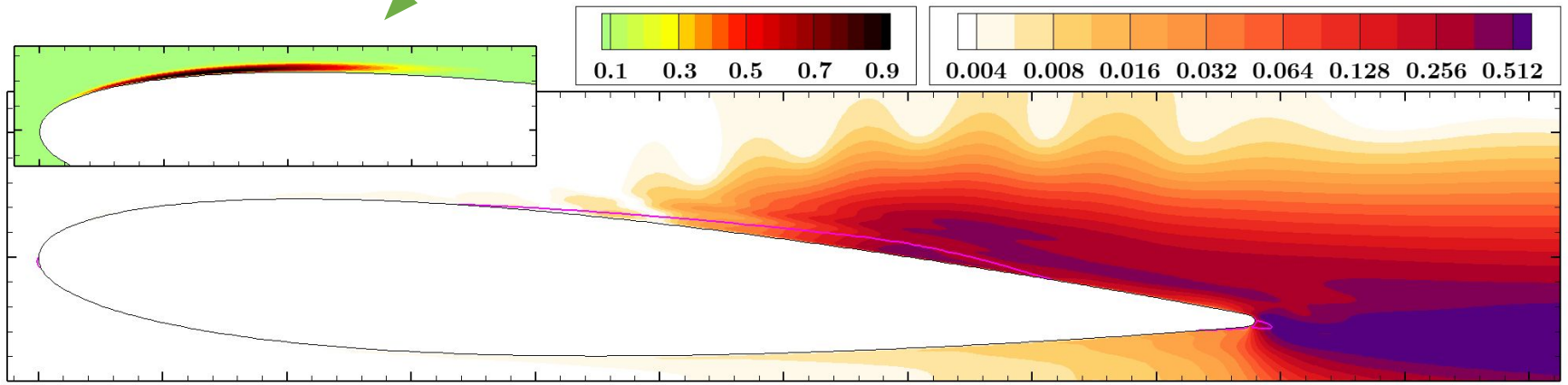
- Non-normality effects due to shear
- Transient growth: interaction of stability modes (non-orthogonal)
- Higher frequencies are more sensitive

Yeh and Taira, JFM 2019; Ribeiro et al, PRF 2020

Resolvent analysis

$$H_w = U\Sigma V^*$$

Optimal forcing



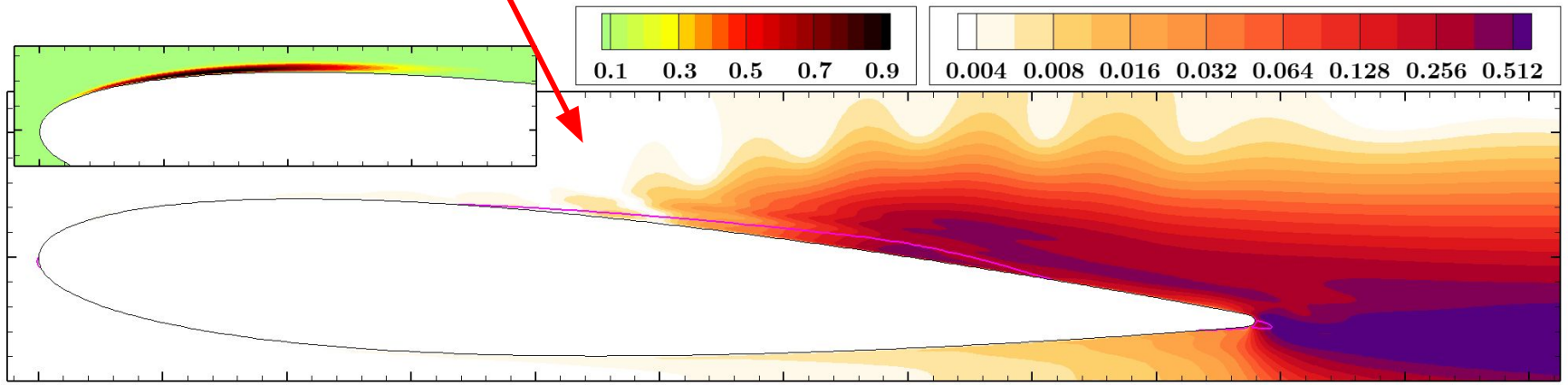
- Magnitude of resolvent modes for kinetic energy
- St ~ 5.1
- Forcing mode (top-left)
- Response mode (bottom-right)

- Forcing occurs through disturbances at the leading edge
- Amplification occurs along separation bubble
- Amplified disturbances reach the trailing edge

Resolvent analysis

$$H_w = \boldsymbol{U}\Sigma\boldsymbol{V}^*$$

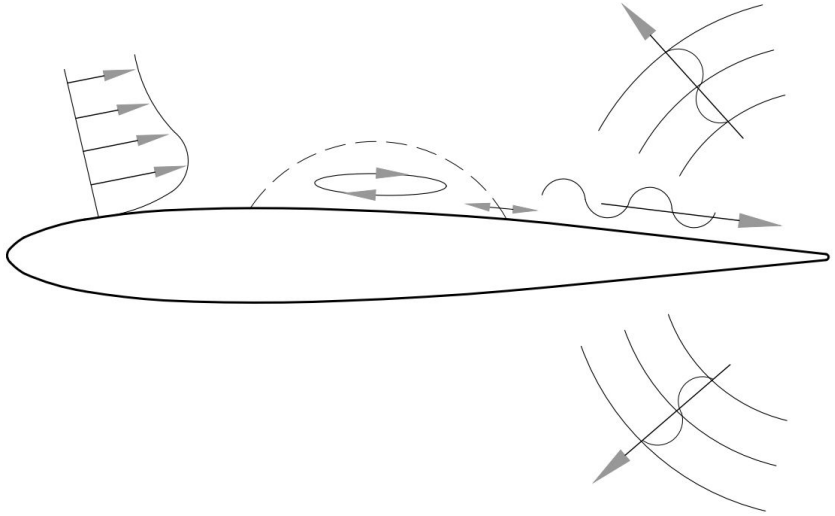
Optimal response



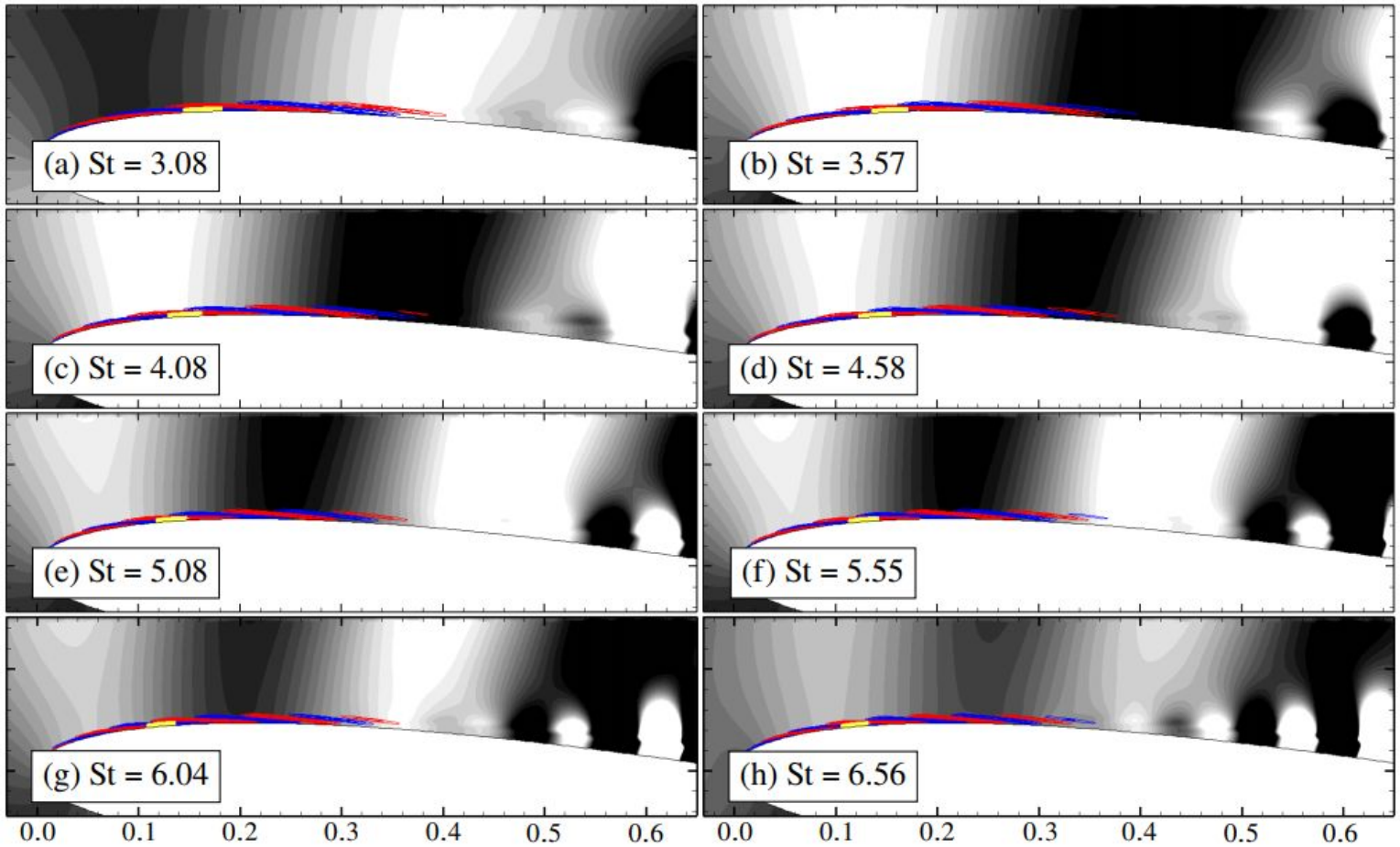
- Magnitude of resolvent modes for kinetic energy
- St ~ 5.1
- Forcing mode (top-left)
- Response mode (bottom-right)

- Forcing occurs through disturbances at the leading edge
- Amplification occurs along separation bubble
- Amplified disturbances reach the trailing edge

Feedback loop mechanism



- Upstream propagating waves trigger feedback loop
- Flow instabilities amplify along the separation bubble
- Vortex merging downstream
- Advection of coherent structures lead to acoustic scattering at the trailing edge



Real component of pressure response (gray scale) and u-velocity forcing (color): yellow spot shows most sensitive region

Matrix-free approach

Stability analysis via mean flow perturbation (MFP) [1,2]

$$\frac{\partial(\bar{\boldsymbol{q}} + \boldsymbol{q}')}{\partial t} = \mathcal{N}(\bar{\boldsymbol{q}} + \boldsymbol{q}')$$

[1] Touber and Sandham, TCFD 2009

[2] Bhaumik et al, AIAA 2015

[3] Ranjan et al, AIAA 2018

Matrix-free approach

Stability analysis via mean flow perturbation (MFP) [1,2]

$$\frac{\partial(\bar{\boldsymbol{q}}+\boldsymbol{q}')}{\partial t} = \mathcal{N}(\bar{\boldsymbol{q}}+\boldsymbol{q}') = \mathcal{N}(\bar{\boldsymbol{q}}) + \frac{\partial \mathcal{N}(\bar{\boldsymbol{q}})}{\partial \boldsymbol{q}}\boldsymbol{q}' + \frac{1}{2}\frac{\partial^2 \mathcal{N}(\bar{\boldsymbol{q}})}{\partial^2 \boldsymbol{q}}\boldsymbol{q}'^2 + \dots$$

Mean flow is not an equilibrium state of NS equations

$$\frac{\partial \boldsymbol{q}'}{\partial t} + \left(\frac{\partial \bar{\boldsymbol{q}}}{\partial t} - \mathcal{N}(\bar{\boldsymbol{q}}) - \mathcal{R}\right) = \frac{\partial \mathcal{N}(\bar{\boldsymbol{q}})}{\partial \boldsymbol{q}}\boldsymbol{q}' + \frac{1}{2}\frac{\partial^2 \mathcal{N}(\bar{\boldsymbol{q}})}{\partial^2 \boldsymbol{q}}\boldsymbol{q}'^2 + \dots$$

[1] Touber and Sandham, TCFD 2009

[2] Bhaumik et al, AIAA 2015

[3] Ranjan et al, AIAA 2018

Matrix-free approach

Stability analysis via mean flow perturbation (MFP) [1,2]

$$\frac{\partial(\bar{\boldsymbol{q}}+\boldsymbol{q}')}{\partial t} = \mathcal{N}(\bar{\boldsymbol{q}}+\boldsymbol{q}') = \mathcal{N}(\bar{\boldsymbol{q}}) + \frac{\partial \mathcal{N}(\bar{\boldsymbol{q}})}{\partial \boldsymbol{q}}\boldsymbol{q}' + \frac{1}{2}\frac{\partial^2 \mathcal{N}(\bar{\boldsymbol{q}})}{\partial^2 \boldsymbol{q}}\boldsymbol{q}'^2 + \dots$$

Mean flow is not an equilibrium state of NS equations

$$\frac{\partial \boldsymbol{q}'}{\partial t} + \left(\frac{\partial \bar{\boldsymbol{q}}}{\partial t} - \mathcal{N}(\bar{\boldsymbol{q}}) - \mathcal{R}\right) = \frac{\partial \mathcal{N}(\bar{\boldsymbol{q}})}{\partial \boldsymbol{q}}\boldsymbol{q}' + \frac{1}{2}\frac{\partial^2 \mathcal{N}(\bar{\boldsymbol{q}})}{\partial^2 \boldsymbol{q}}\boldsymbol{q}'^2 + \dots$$

$= 0$

if base flow is stationary

[1] Touber and Sandham, TCFD 2009

[2] Bhaumik et al, AIAA 2015

[3] Ranjan et al, AIAA 2018

Matrix-free approach

Stability analysis via mean flow perturbation (MFP) [1,2]

$$\frac{\partial(\bar{\boldsymbol{q}}+\boldsymbol{q}')}{\partial t} = \mathcal{N}(\bar{\boldsymbol{q}}+\boldsymbol{q}') = \mathcal{N}(\bar{\boldsymbol{q}}) + \frac{\partial \mathcal{N}(\bar{\boldsymbol{q}})}{\partial \boldsymbol{q}}\boldsymbol{q}' + \frac{1}{2}\frac{\partial^2 \mathcal{N}(\bar{\boldsymbol{q}})}{\partial^2 \boldsymbol{q}}\boldsymbol{q}'^2 + \dots$$

Mean flow is not an equilibrium state of NS equations

$$\frac{\partial \boldsymbol{q}'}{\partial t} + \left(\frac{\partial \bar{\boldsymbol{q}}}{\partial t} - \mathcal{N}(\bar{\boldsymbol{q}}) - \mathcal{R}\right) = \frac{\partial \mathcal{N}(\bar{\boldsymbol{q}})}{\partial \boldsymbol{q}}\boldsymbol{q}' + \frac{1}{2}\frac{\partial^2 \mathcal{N}(\bar{\boldsymbol{q}})}{\partial^2 \boldsymbol{q}}\boldsymbol{q}'^2 + \dots$$

$= 0$ if base flow is stationary

~ 0 small perturbations

[1] Touber and Sandham, TCFD 2009

[2] Bhaumik et al, AIAA 2015

[3] Ranjan et al, AIAA 2018

Matrix-free approach

Stability analysis via mean flow perturbation (MFP) [1,2]

$$\frac{\partial(\bar{\boldsymbol{q}}+\boldsymbol{q}')}{\partial t} = \mathcal{N}(\bar{\boldsymbol{q}}+\boldsymbol{q}') = \mathcal{N}(\bar{\boldsymbol{q}}) + \frac{\partial \mathcal{N}(\bar{\boldsymbol{q}})}{\partial \boldsymbol{q}}\boldsymbol{q}' + \frac{1}{2}\frac{\partial^2 \mathcal{N}(\bar{\boldsymbol{q}})}{\partial^2 \boldsymbol{q}}\boldsymbol{q}'^2 + \dots$$

Mean flow is not an equilibrium state of NS equations

$$\frac{\partial \boldsymbol{q}'}{\partial t} + \left(\frac{\partial \bar{\boldsymbol{q}}}{\partial t} - \mathcal{N}(\bar{\boldsymbol{q}}) - \mathcal{R}\right) = \frac{\partial \mathcal{N}(\bar{\boldsymbol{q}})}{\partial \boldsymbol{q}}\boldsymbol{q}' + \frac{1}{2}\frac{\partial^2 \mathcal{N}(\bar{\boldsymbol{q}})}{\partial^2 \boldsymbol{q}}\boldsymbol{q}'^2 + \dots$$

$= 0$ if base flow is stationary

~ 0 small perturbations

Time evolution of disturbances

$$\frac{\partial \boldsymbol{q}'}{\partial t} \approx \frac{\partial \mathcal{N}(\bar{\boldsymbol{q}})}{\partial \boldsymbol{q}}\boldsymbol{q}' = \boldsymbol{L}\boldsymbol{q}'$$

Initial condition: impulse excitation [3]

MFP accounts for modal interaction and transient energy amplification

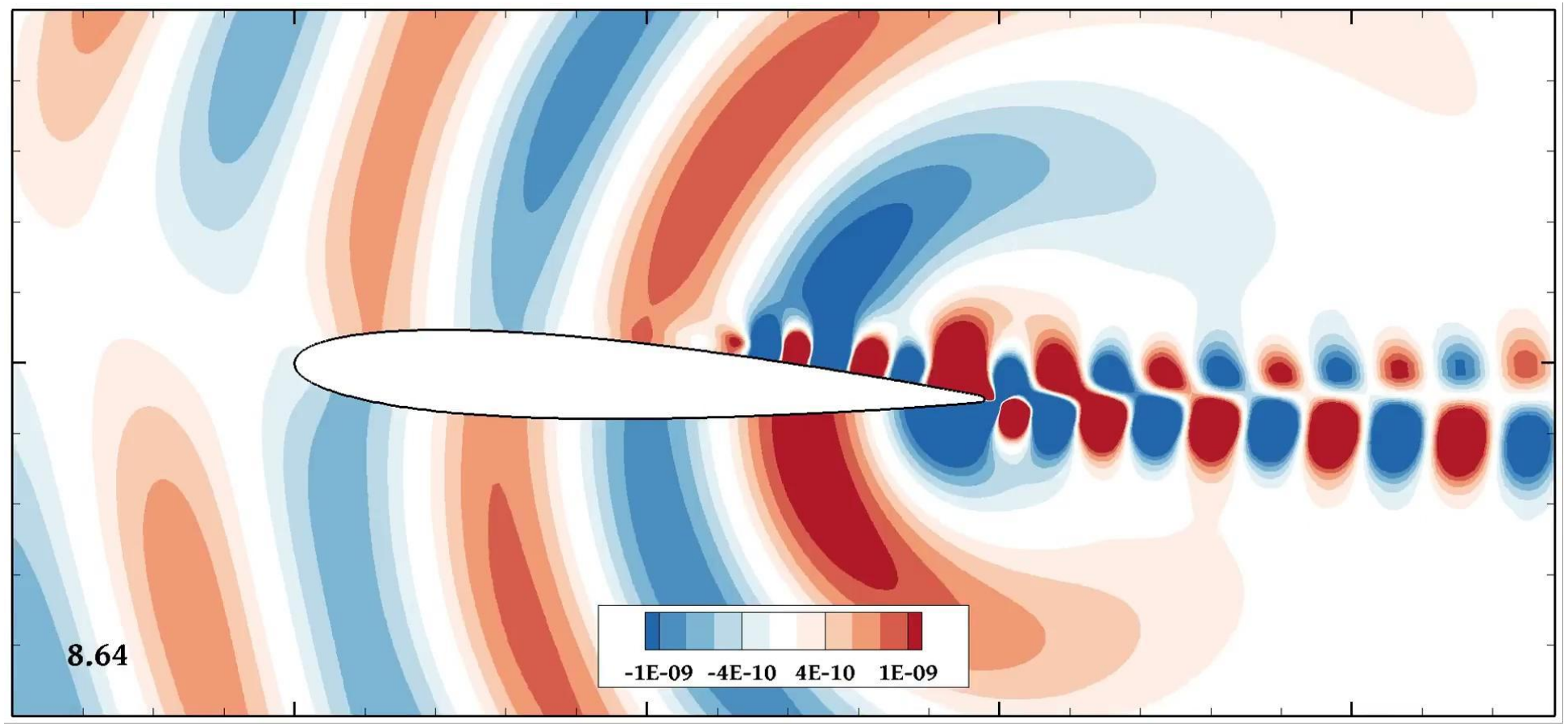
[1] Touber and Sandham, TCFD 2009

[2] Bhaumik et al, AIAA 2015

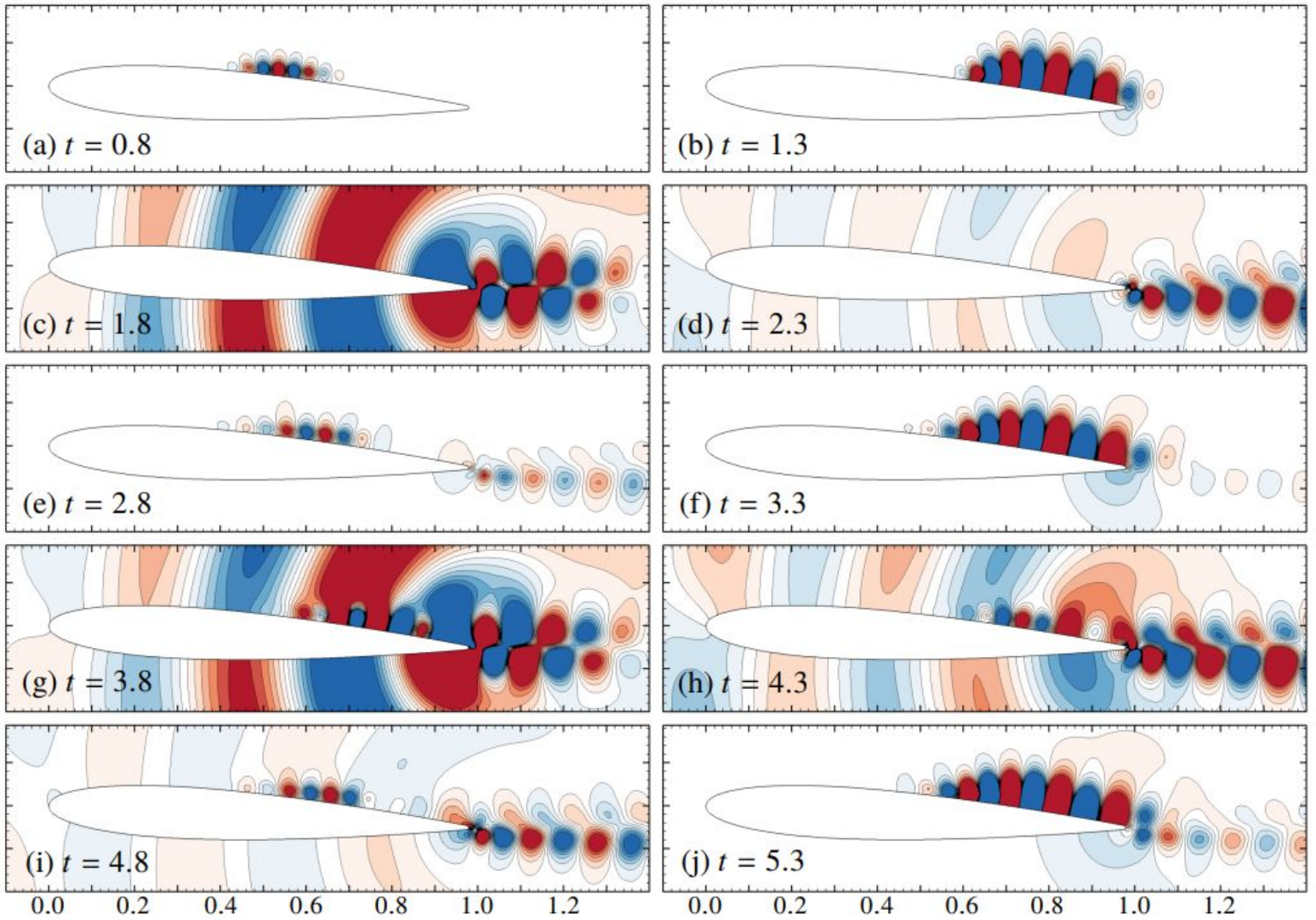
[3] Ranjan et al, AIAA 2018

Back to acoustic feedback!

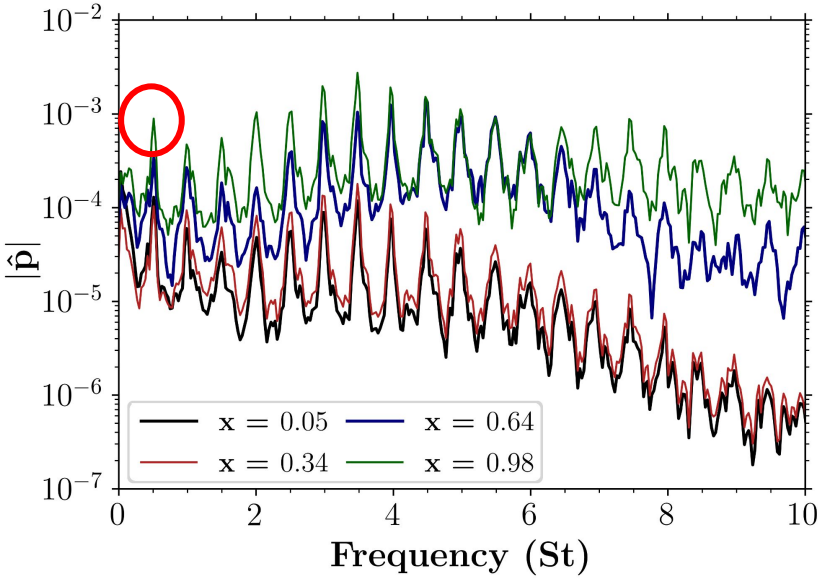
Linear evolution of disturbances



Back to acoustic feedback!



- Snapshots of linearized NS eqs.
- Pressure fluctuations
- Wavepackets composed of multiple frequencies generated at $\Delta t = 2.0$ (lowest tone from spectrum)
- Acoustic scattering triggers new wavepackets

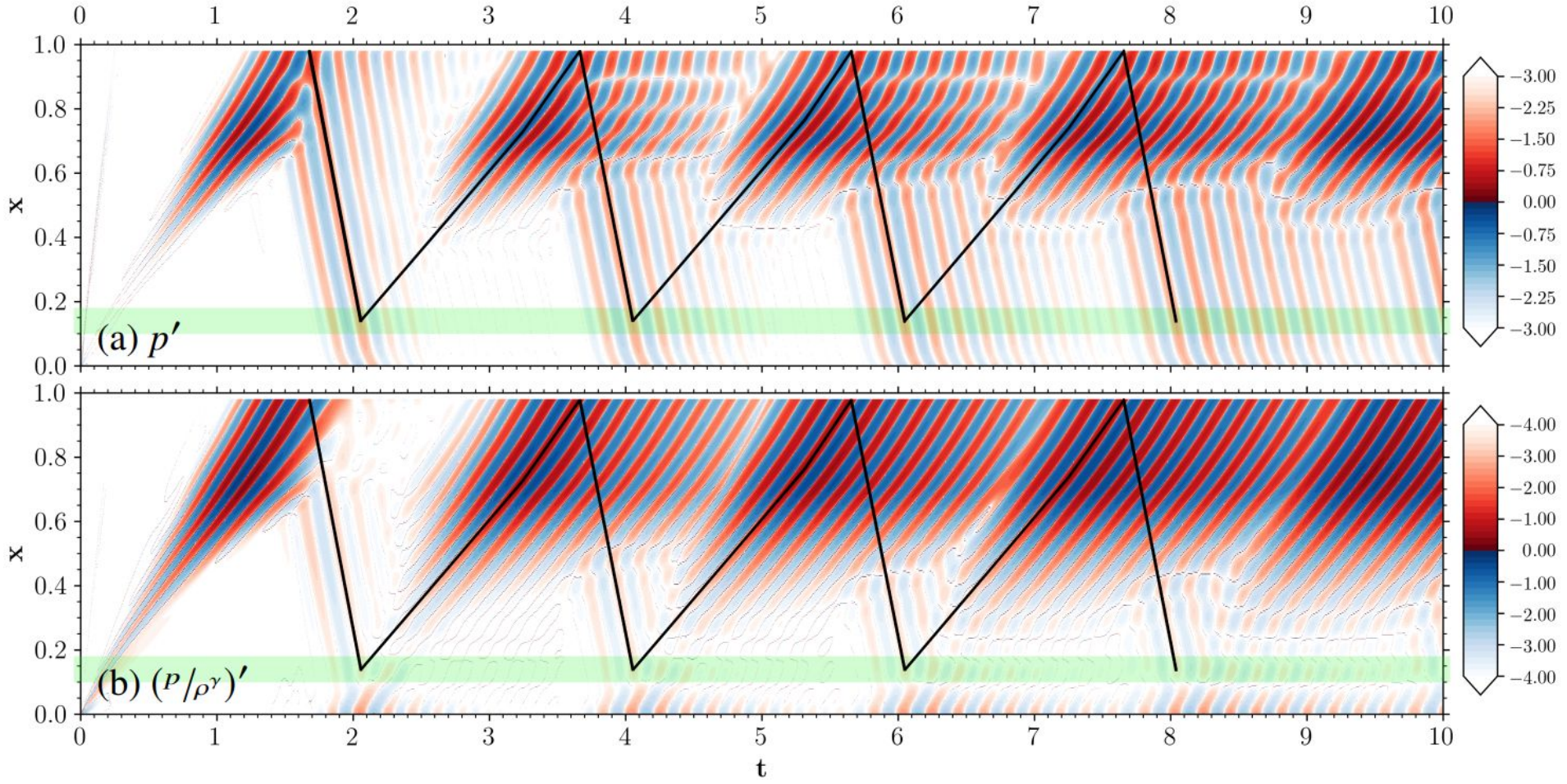


Acoustic feedback

Space-time map of linear solution from MFP

Acoustic fluctuations

Entropy fluctuations



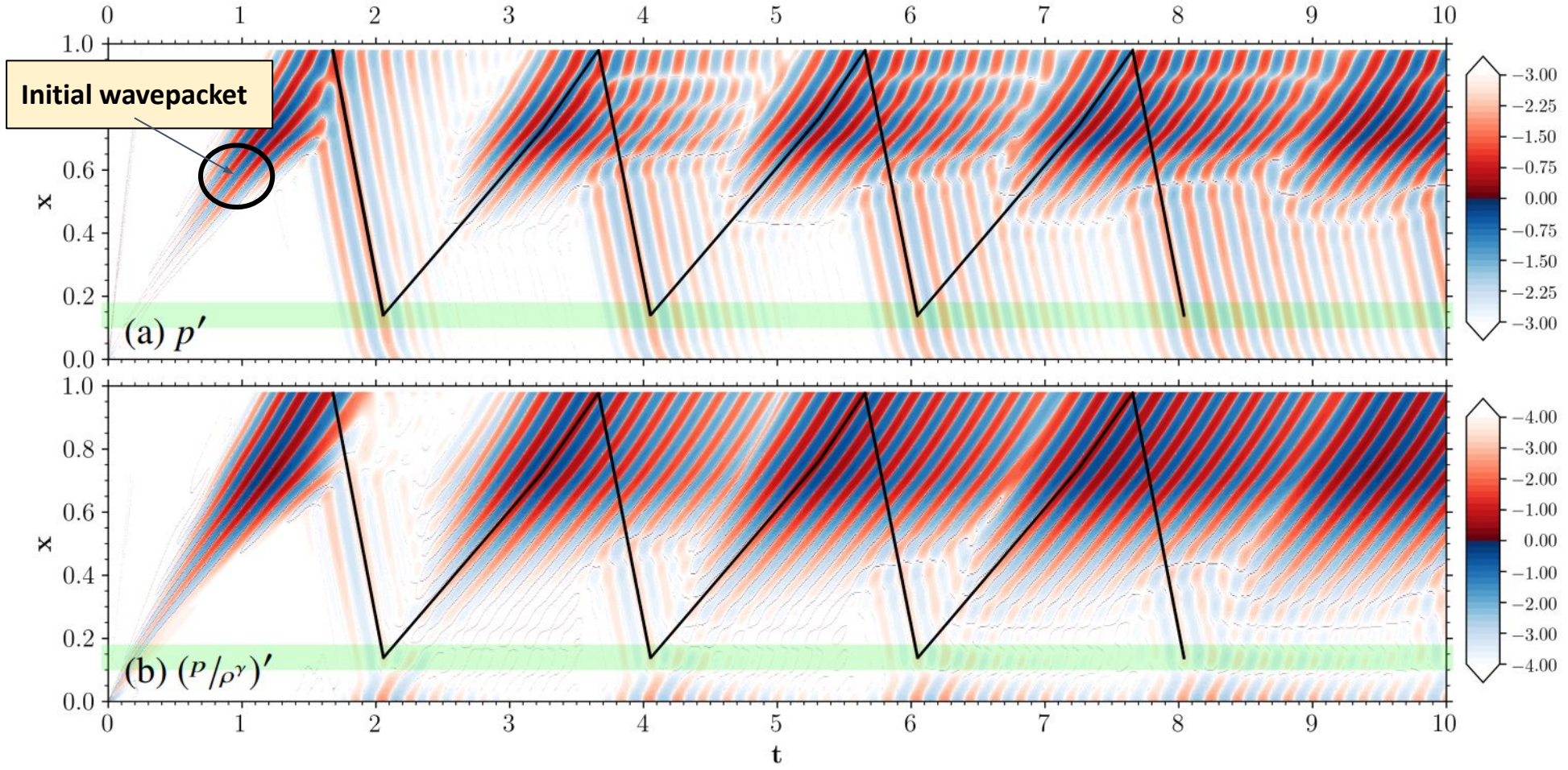
Log scale

Acoustic feedback

Space-time map of linear solution from MFP

Acoustic fluctuations

Entropy fluctuations



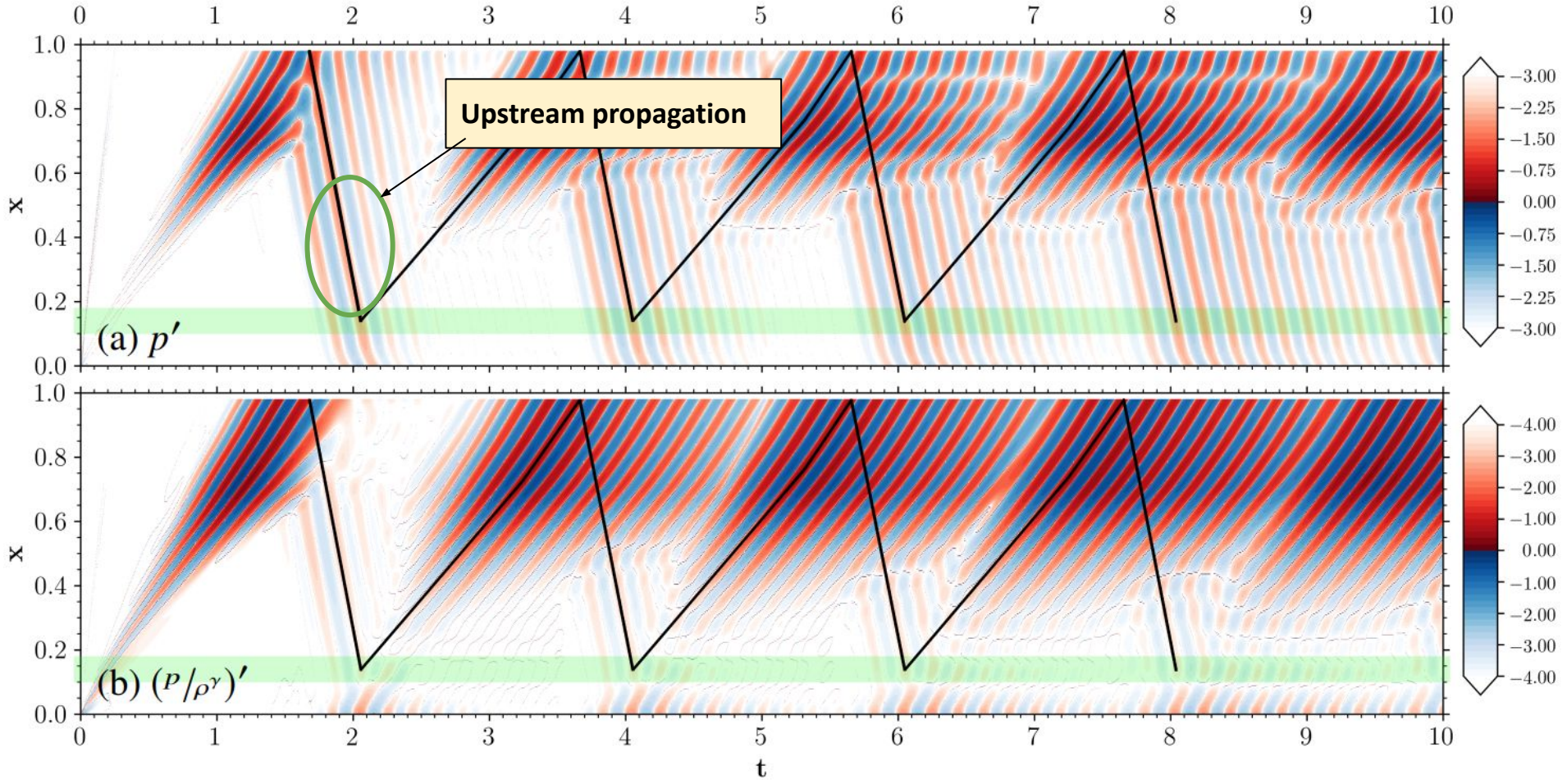
Log scale

Acoustic feedback

Space-time map of linear solution from MFP

Acoustic fluctuations

Entropy fluctuations



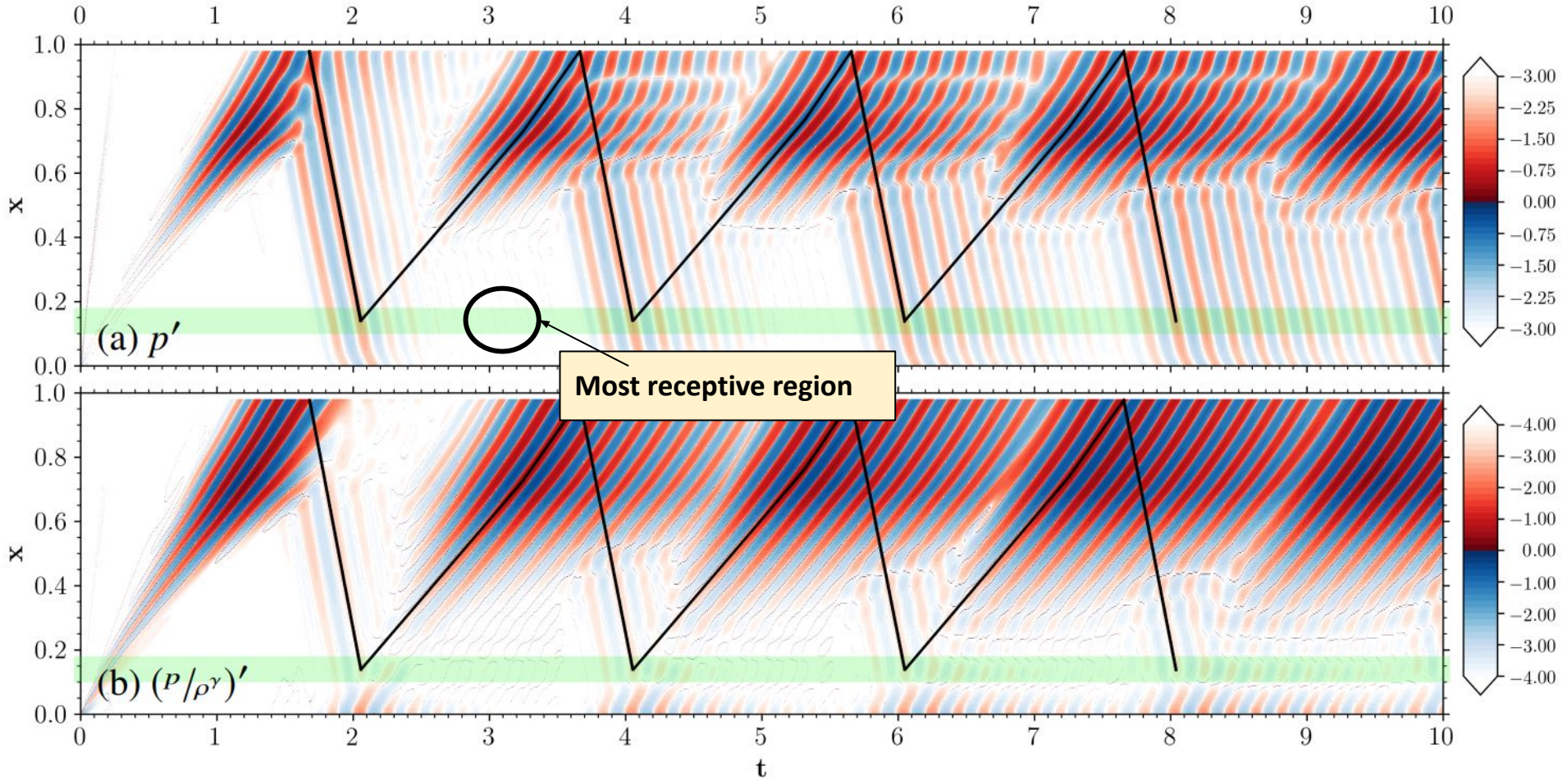
Log scale

Acoustic feedback

Space-time map of linear solution from MFP

Acoustic fluctuations

Entropy fluctuations

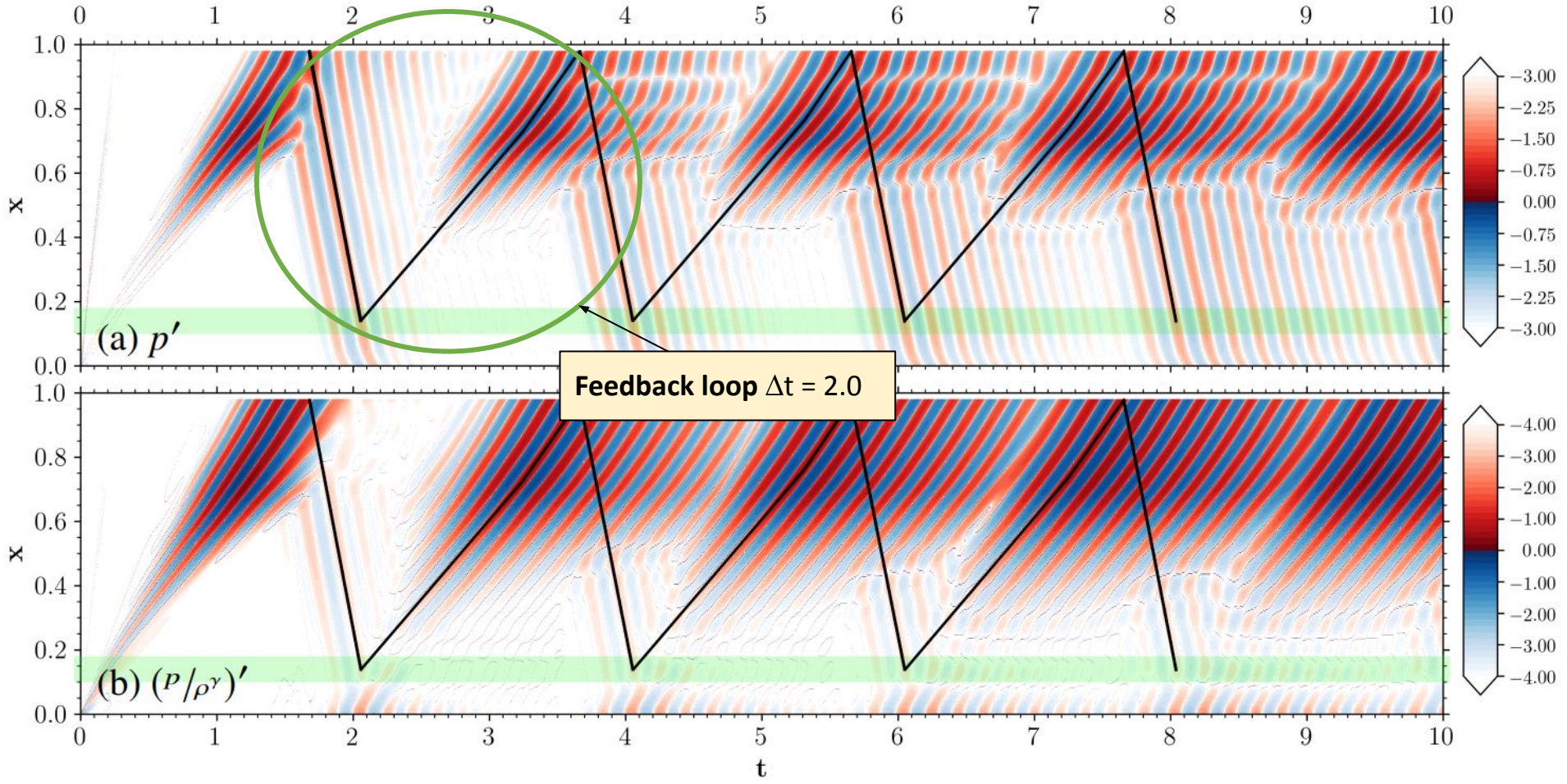


Acoustic feedback

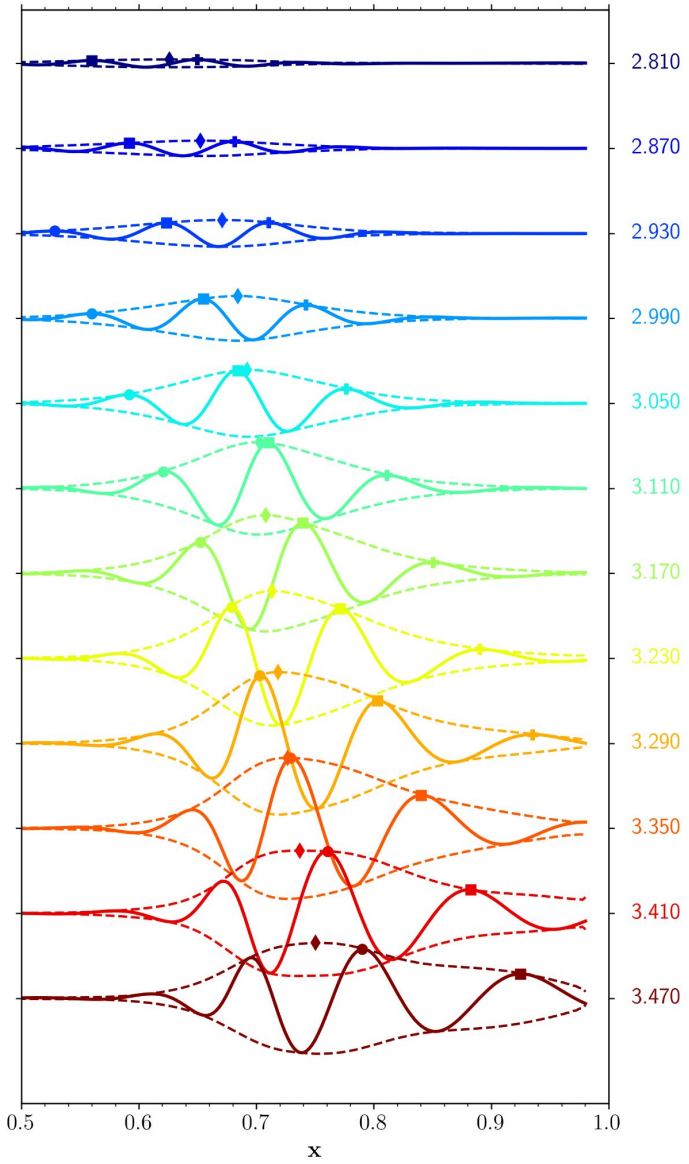
Space-time map of linear solution from MFP

Acoustic fluctuations

Entropy fluctuations

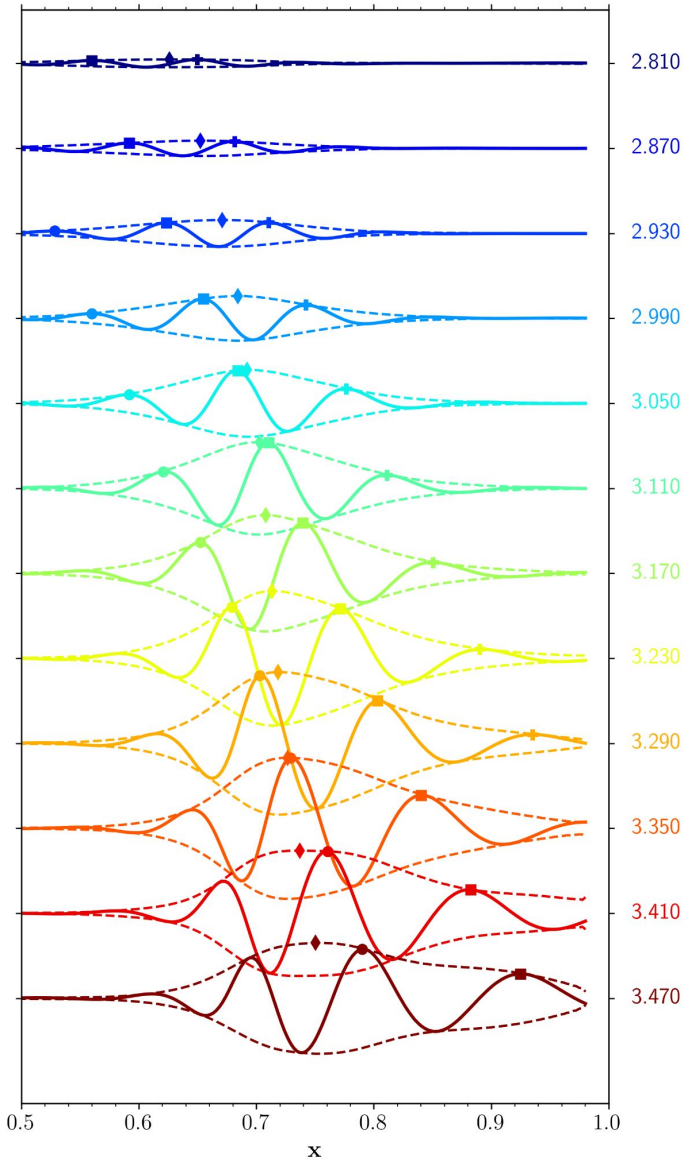


Wavepacket dynamics

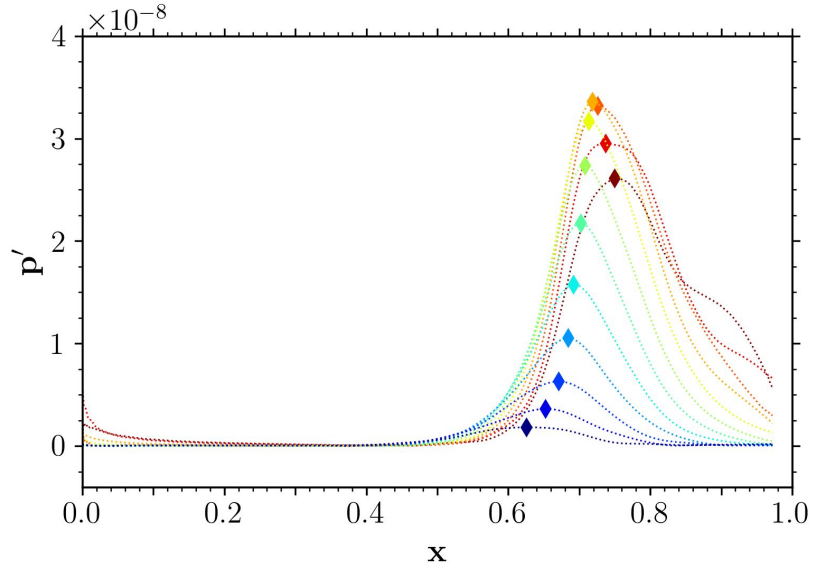


- Spatio-temporal evolution of wavepacket computed with Hilbert transform
- Diamond symbols marks envelope: group velocity
- Square and circle marks wave crests: phase velocity

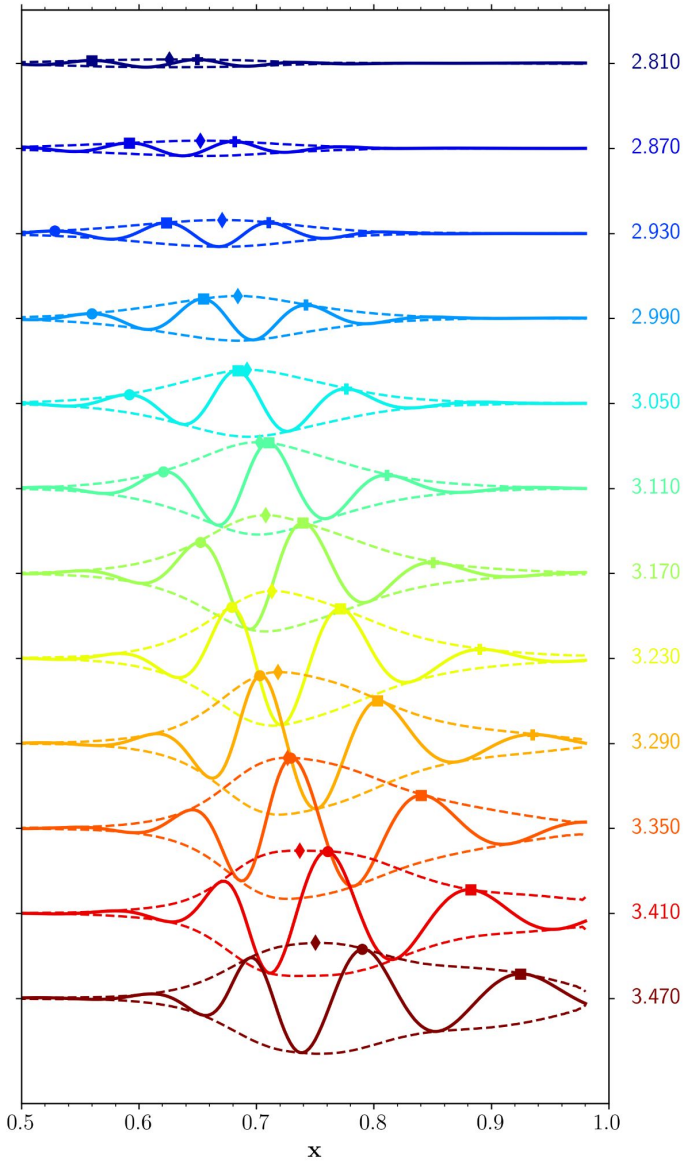
Wavepacket dynamics



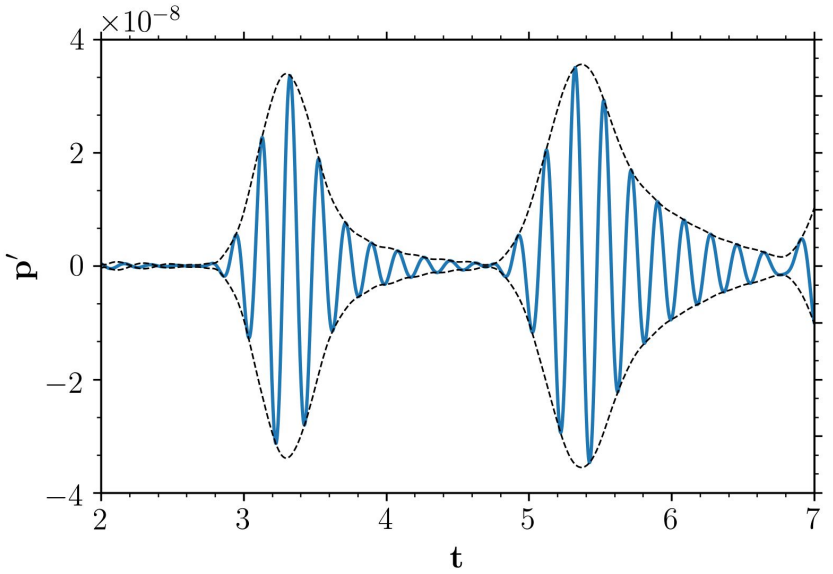
- Spatial shape of wavepacket
- Diamond symbols marks envelope: group velocity

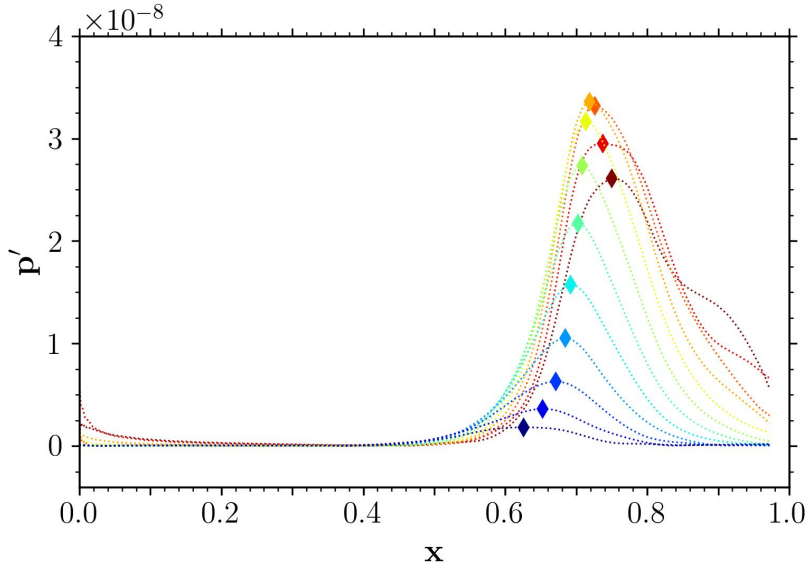


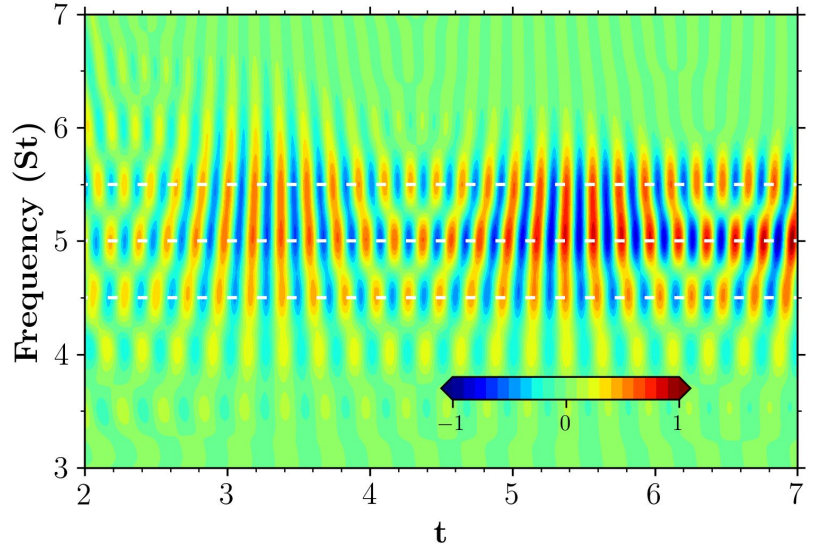
Wavepacket dynamics



- Spatial shape of wavepacket
- Temporal signal
- Scalogram at point of maximum amplitude provides phase information of envelopes
- Energy amplification depends on constructive interference of multiple modes







Acoustic feedback one more time!

Space-time map of integral length scale computed from two-point correlations

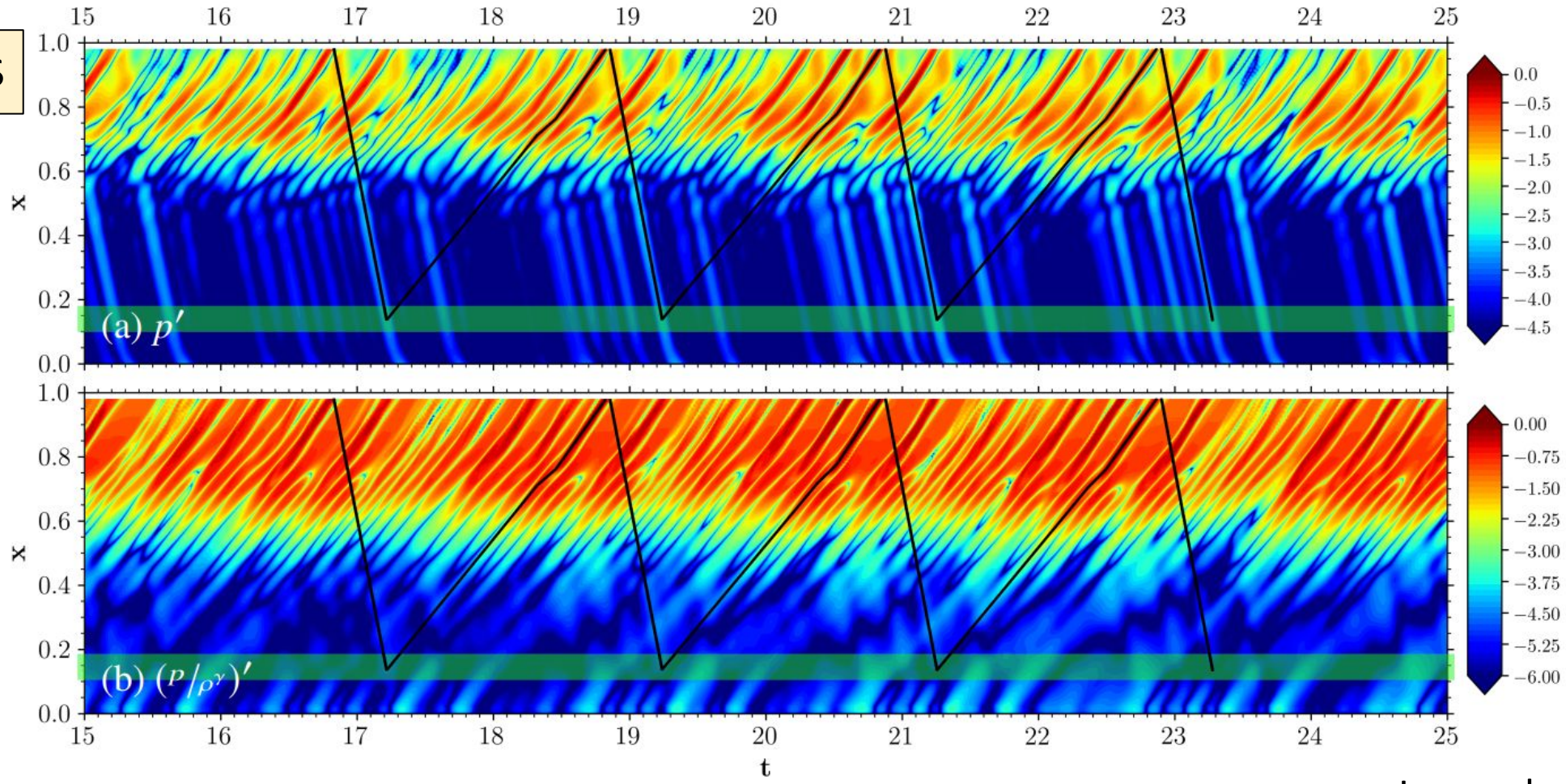
Results obtained from LES

Pressure

- acoustic waves radiate upstream
- hydrodynamic **p'** advected downstream the bubble

Entropy

- partial filtering of acoustic waves
- feedback loop closes near the leading edge



Log scale

The role of phase

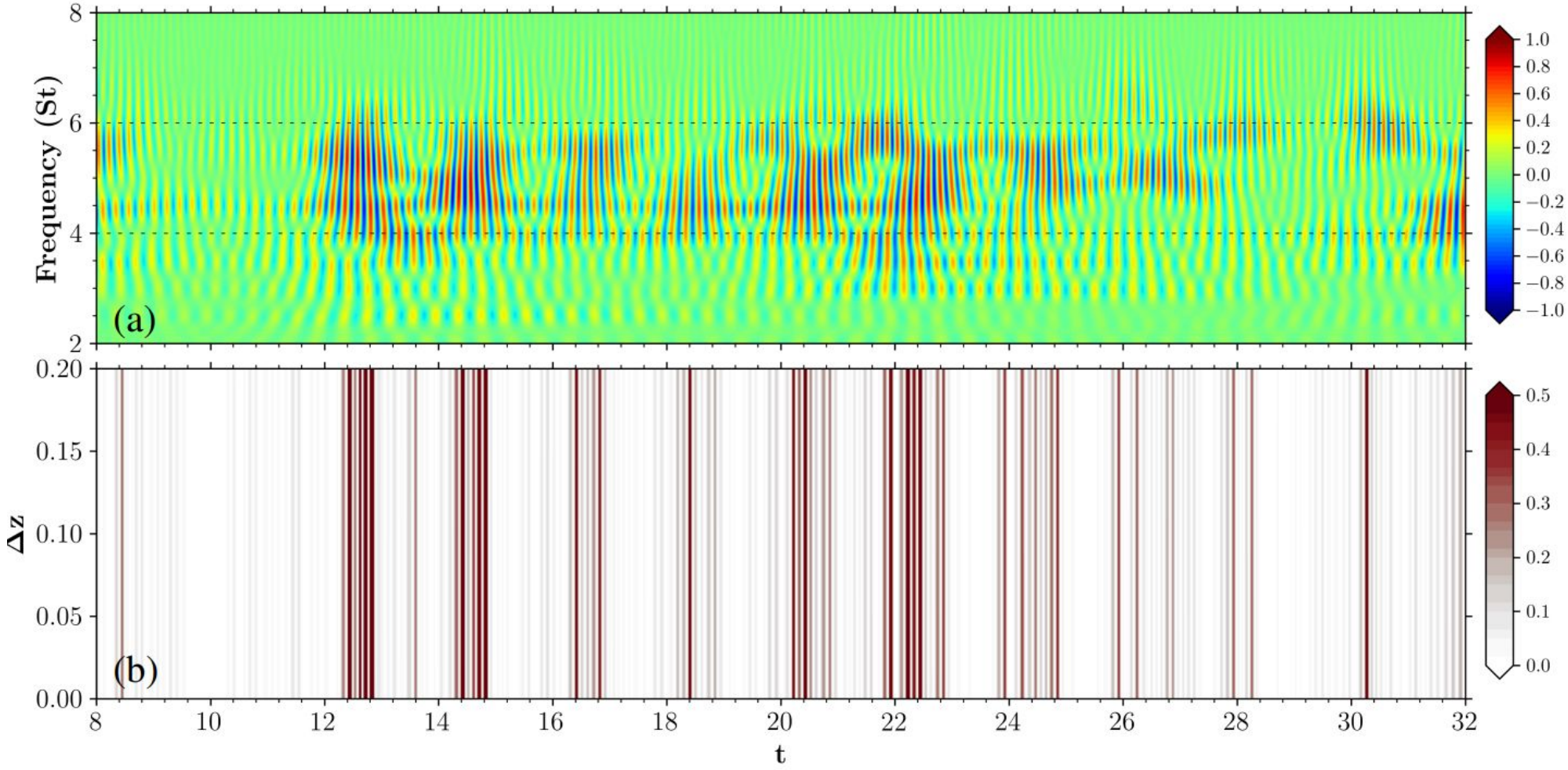
Spanwise pressure correlation at x = 0.64 (inside separation bubble before merging)

Phase information

4 < St < 6
Most amplified frequencies in linear analysis

Green spots: turbulence

Phase alignment: stronger coherence



Conclusions

- Study of airfoil noise at combining LES and linear analysis (LST and resolvent)
- Focus on secondary tones and acoustic feedback loop
- Three-dimensional effects are previously neglected in most numerical studies (role of transition to turbulence)
- Main tone plus secondary tones are still present despite intermittent transition
- Magnitude of acoustic waves depends on spanwise coherence of vortical structures
- Dominant tone related to the frequency of shedding with secondary tones induced by amplitude and phase modulation from separation bubble

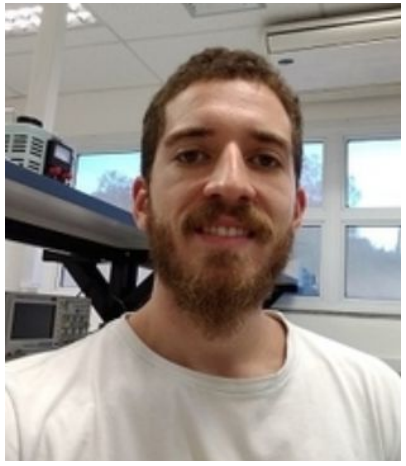
Conclusions

- Linear stability analysis indicates that overall flow dynamics originates from linear mechanisms
- Leading edge region is more receptive to disturbances and separation bubble acts as an amplifier
- Vortex dynamics may lead to either solitary or merged vortices and phase alignment controls coherence
- Acoustic feedback loop is observed in both linear and nonlinear analyses
- Intensity of acoustic waves depends on spanwise coherence of vortical structures
- Intermittency from laminar-turbulent transition affects the feedback loop

Current work on flow control

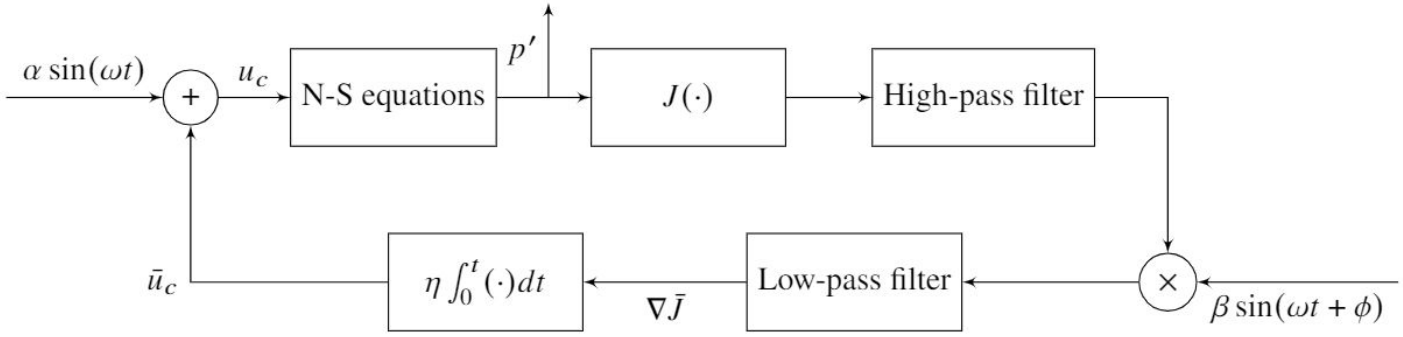
Airfoil noise reduction with closed-loop active flow control

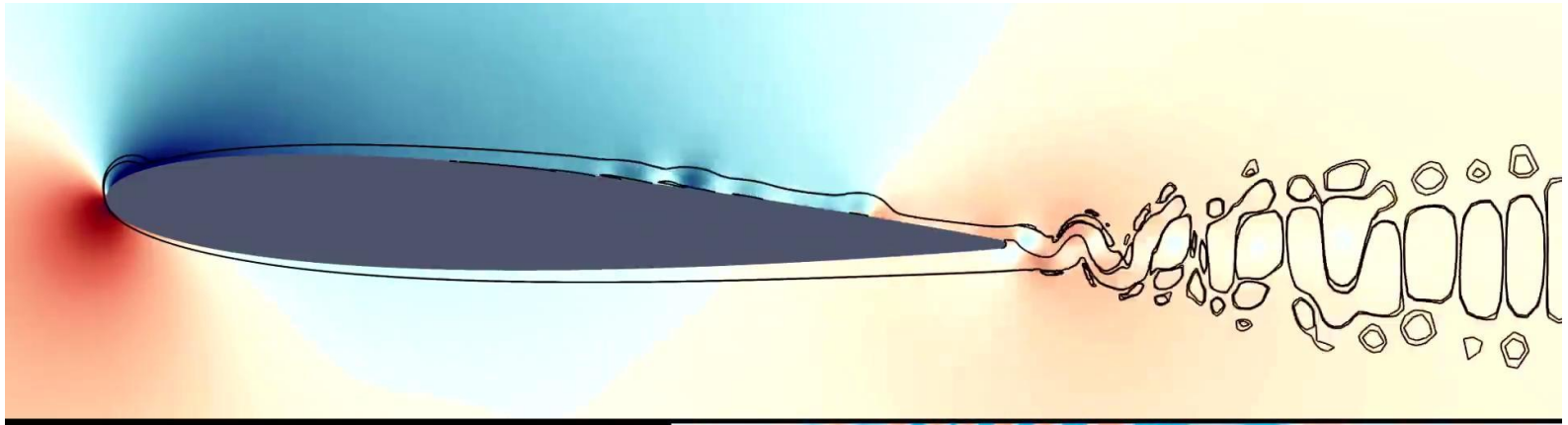
Extremum seeking control (ESC) and slope seeking control
Déda and Wolf AIAA 2021

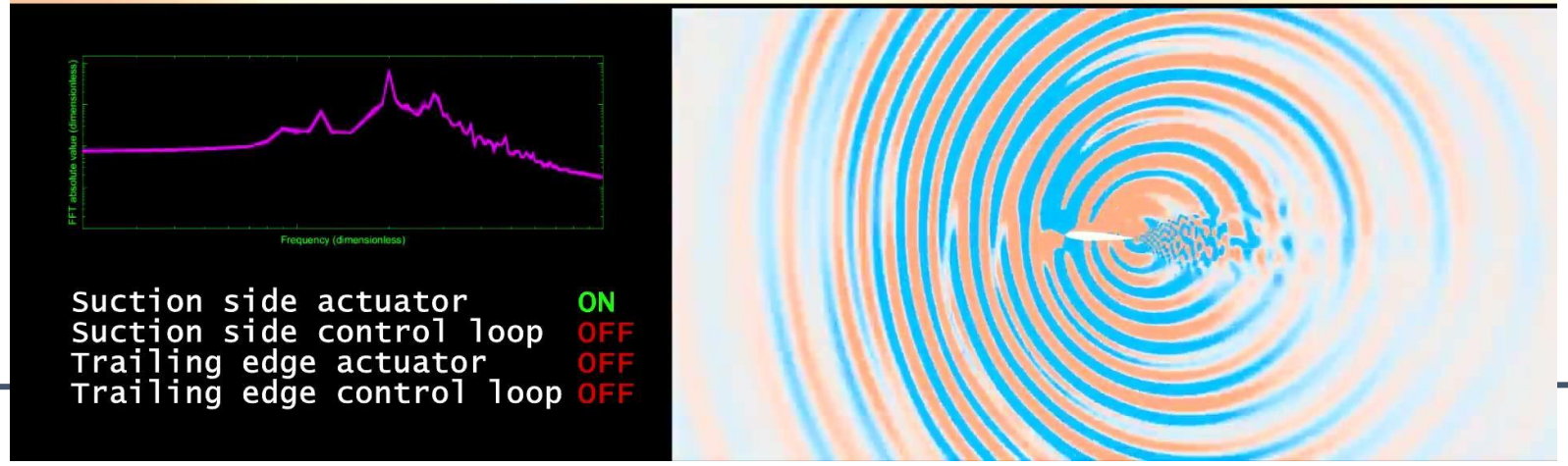


ESC module implemented on CFD code

ESC seeks to minimize noise emission in real-time







Acknowledgements

Prof. Chi-An Yeh, Jean Ribeiro

Thank You!

Questions?

Large eddy simulation and linear analysis of an airfoil in transitional flow: Insights on secondary tones and acoustic feedback







Tulio Ricciardi **William Wolf** **Kunihiko Taira**

University of Campinas

University of California Los Angeles

Advanced Modeling & Simulation (AMS) Seminar, June 10th, 2021